

## Regular Article

# *Metformin is a Superior Substrate for Renal Organic Cation Transporter OCT2 rather than Hepatic OCT1*

Naoko KIMURA, Satohiro MASUDA, Yuko TANIHARA, Harumasa UEO,  
Masahiro OKUDA, Toshiya KATSURA and Ken-ichi INUI

Department of Pharmacy, Kyoto University Hospital, Faculty of Medicine, Kyoto University, Kyoto, Japan

Full text of this paper is available at <http://www.jstage.jst.go.jp/browse/dmpk>

**Summary:** Although metformin, a cationic agent for type II diabetes, shows its pharmacological effect in the liver, the drug is mainly eliminated into urine. The tissue selectivity based on the function of drug transporters is unclear. In the present study, the transport of metformin was examined using HEK293 cells transiently transfected with five human renal organic ion transporter cDNAs. Human OCT1 and OCT2, but not OAT1, OAT3 or OCT2-A, stimulated the uptake. A kinetic analysis of metformin transport demonstrated that the amount of plasmid cDNA for transfection was also important parameter to the quantitative elucidation of functional characteristics of transporters, and both human and rat OCT2 had about a 10- and 100-fold greater capacity to transport metformin than did OCT1, respectively. In male rats, the mRNA expression level of rOCT2 in the whole kidneys was 8-fold greater than that of rOCT1 in the whole liver. The *in vivo* distribution of metformin in rats revealed that the expression level of renal OCT2 was a key factor in the control of the concentrative accumulation of metformin in the kidney. These findings suggest that metformin is a superior substrate for renal OCT2 rather than hepatic OCT1, and renal OCT2 plays a dominant role for metformin pharmacokinetics.

**Key words:** organic cation transporter; kidney; liver; diabetes; biguanide; TEA

### Introduction

Tissue-specific organic cation transporters contribute to the hepatic- or renal-selective distribution of cationic compounds including endogenous substrates, drugs, and their metabolites. Gründemann *et al.*<sup>1)</sup> isolated a rat organic cation transporter, rOCT1 (slc22a1), which was preferentially expressed in the liver and kidney. We isolated rOCT2 (slc22a2) which was homologous to rOCT1, and found that its mRNA was solely expressed in the kidney.<sup>2)</sup> In humans, OCT1 (SLC22A1) is primarily expressed in the liver,<sup>3)</sup> and the human

(h)OCT1 could not be detected in the human kidney.<sup>4)</sup> In addition, hOCT2 (SLC22A2) was found to be the most abundant organic cation transporter in the basolateral membranes of human kidney.<sup>4)</sup> Because OCT1 and OCT2 were similar in substrate specificity, it had been difficult to explain the difference in the tissue distribution of cationic drugs between liver and kidney.<sup>5)</sup>

One of the biguanide agents, metformin, is extensively excreted into urine, mostly via the tubular secretion.<sup>6)</sup> However, it has been considered that the pharmacological target organ is the liver, and the lactic acidosis is one of the severe side effects of the drug. Wang *et al.*<sup>7)</sup> reported that the OCT1 mediated the intestinal and hepatic distribution of metformin in rats and mice. The relation between the OCT1 expression and lactic acidosis was reported by use of OCT1 null mice.<sup>8)</sup> Using the electrophysiological technique in *Xenopus* oocytes, Dresser *et al.*<sup>9)</sup> suggested that metformin and phenformin interacted with hOCT1 and hOCT2. Recently, we demonstrated that metformin was a substrate for the renal OCT2.<sup>10)</sup> However, there is no

This work was supported in part by a grant-in-aid for Research on Advanced Medical Technology from the Ministry of Health, Labor and Welfare of Japan, by a Japan Health Science Foundation "Research on Health Sciences Focusing on Drug Innovation", by a grant-in-aid for Scientific Research from the Ministry of Education, Science, Culture and Sports of Japan, and by the 21<sup>st</sup> Century COE program "Knowledge Information Infrastructure for Genome Science". H. Ueo was supported as a Teaching Assistant by the 21<sup>st</sup> Century COE program "Knowledge Information Infrastructure for Genome Science".

Received; July 25, 2005, Accepted; August 29, 2005

To whom correspondence should be addressed: Prof. Ken-ichi INUI, Ph.D., Department of Pharmacy, Kyoto University Hospital, Sakyo-ku, Kyoto 606-8507, Japan. Tel. +81-75-751-3577, Fax. +81-75-751-4207, E-mail: [inui@kuhp.kyoto-u.ac.jp](mailto:inui@kuhp.kyoto-u.ac.jp)

information about the contribution of OCT1 and OCT2 on the *in vivo* pharmacokinetics of metformin. The quantitative characteristics of metformin transport by OCT1 or OCT2 are needed to understand the hepatic or renal selectivity of metformin.

In the present study, the quantitative analyses for metformin transport activity, using the limited amount of transfected cDNA, have been performed to clarify the difference in the transport capacity as well as the substrate affinity between OCT1 and OCT2 using both the human and rat clones. The results clearly revealed that metformin was a superior substrate for the renal OCT2 rather than hepatic OCT1.

### Methods

**Materials:** [Biguanidine-<sup>14</sup>C]metformin hydrochloride (26 mCi/mmol) was purchased from Moravек Biochemicals, Inc. (Brea, CA). Metformin and 1-methyl-4-phenylpyridinium iodide were obtained from Sigma-Aldrich Co. (St. Louis, MO). All other compounds used were of the highest purity available.

**Cell culture and transfection:** HEK 293 cells (ATCC CRL-1573, American Type Culture Collection, Manassas, VA) were cultured in complete medium consisting of Dulbecco's modified Eagle's medium with 10% fetal bovine serum in an atmosphere of 5% CO<sub>2</sub>/95% air at 37°C, and used as host cells. pCMV6-XL4 plasmid vector (OriGene Technologies, Rockville, MD) DNA (800 ng) containing hOCT1, hOCT2, and hOCT2-A cDNA, and pBK-CMV vector (Stratagene, La Jolla, CA) DNA (800 ng) containing hOAT1, hOAT3, rOCT1, and rOCT2 cDNA were used to conduct the transient expression analysis, as described.<sup>11)</sup> The transfectant stably expressing hOCT1 was established as described previously.<sup>10,12)</sup> The cell monolayers were used at day 3 of culture for uptake experiments.

**Uptake experiments:** Cellular uptake of cationic compounds was measured with monolayer cultures of HEK293 cells grown on poly-D-lysine-coated 24-well plates.<sup>10,12)</sup> The incubation medium for uptake experiments contained: 145 mM NaCl, 3 mM KCl, 1 mM CaCl<sub>2</sub>, 0.5 mM MgCl<sub>2</sub>, 5 mM D-glucose, and 5 mM HEPES (pH 7.4). The pH of the medium was adjusted with NaOH or HCl. The cells were preincubated with 0.2 mL of incubation medium for 10 min at 37°C. The medium was then removed, and 0.2 mL of incubation medium containing [<sup>14</sup>C]metformin or [ethyl-<sup>14</sup>C]tetraethylammonium (TEA) bromide was added. The medium was aspirated off at the end of the incubation, and the monolayers were rapidly rinsed

twice with 1 mL of ice-cold incubation medium. The cells were solubilized in 0.5 mL of 0.5N NaOH, and then the radioactivity in aliquots was determined by liquid scintillation counting. The protein content of the solubilized cells was determined by the method of Bradford,<sup>13)</sup> using a Bio-Rad Protein Assay Kit (Bio-Rad Laboratories, Hercules, CA) with bovine  $\gamma$ -globulin as a standard.

**mRNA expression of organic cation transporters:** The expression levels of hOCT1, hOCT2, rOCT1, and rOCT2 in HEK293 transfectants were quantified as described previously with some modifications.<sup>4)</sup> Briefly, total cellular RNA was isolated from specimens using a MagNA Pure LC RNA isolation Kit II (Roche Diagnostic GmbH, Mannheim, Germany) and was reverse-transcribed to cDNA. Real-time polymerase chain reaction (PCR) was performed using the ABI prism 7700 sequence detector (Applied Biosystems, Foster, CA). Glyceraldehyde-3-phosphate dehydrogenase mRNA was also measured as an internal control with glyceraldehyde-3-phosphate dehydrogenase Control Reagent (Applied Biosystems).

For quantification of the organic cation transporter mRNAs in the whole liver or kidneys in rats, we harvested each tissue from Wistar male rats weighing between 300 g and 330 g (12 weeks old, n=4), and the isolated whole liver or kidneys were minced and incubated in the RNA Later<sup>®</sup> (QIAGEN GmbH, Hilden, Germany) for 10 hours at 4°C. After re-mincing the tissues, a part of the mixed tissue samples were subjected to total RNA extraction. The total RNA extraction, reverse-transcription and real-time PCR were performed as described above.

**In Vivo intravenous administration study:** The animal experiments were performed in accordance with the *Guidelines for Animal Experiments of Kyoto University*. Male and Female Wistar/ST rats weighing 210–240 g were anesthetized with sodium pentobarbital and the femoral artery and vein were cannulated with polyethylene tubing. Tracer amounts of metformin (1 mg/kg) dissolved in saline were administered as a bolus *via* the catheterized right femoral vein. Blood samples were collected at 0.5, 1, 1.5, 2, 2.5, and 3 min from the left femoral artery. Three minutes after the injection, the kidneys and livers were collected immediately after sacrifice. The excised tissues were gently washed, weighed, and homogenized in 3 volumes of saline.<sup>14)</sup> Aliquots (100  $\mu$ L) of blood and tissue homogenates were deproteinized with methanol (200  $\mu$ L) and then subjected to HPLC.

**HPLC analysis:** A high-performance liquid chromatograph LC-10AD (Shimadzu Co., Kyoto, Japan) was equipped with an UV spectrophotometric detector (SPD-100A; Shimadzu Co.) adjusted to 236 nm for metformin and integrator (Chromatopac C-R8A;

The accession numbers of cDNAs used in the present study were as follows: hOCT1, X98332; hOCT2, X98333; hOCT2-A, AB075951; hOAT1, AB009698; hOAT3, AF097491; rOCT1, X78855; rOCT2, D83044.

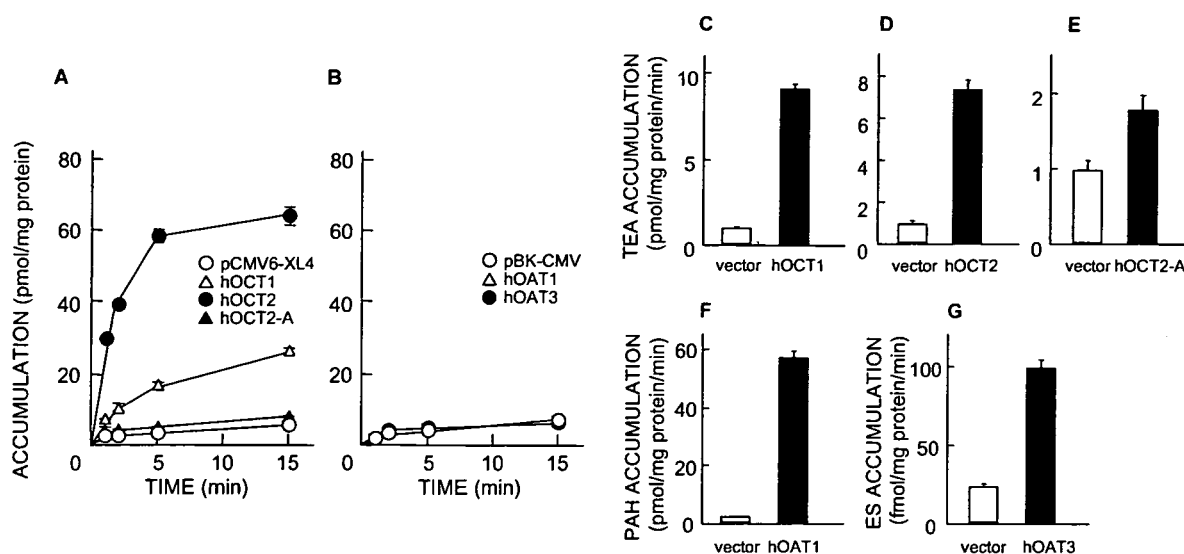


**Fig. 1.** Transport activity for [ $^{14}\text{C}$ ]Metformin by HEK293 cells transiently expressing human organic ion transporters.

(A) HEK293 cells transfected with pCMV6-XL4 vector (open circle), hOCT1 (open triangle), hOCT2 (closed circle), or hOCT2-A (closed triangle) were incubated for the specified periods at 37°C with 0.2 mL of 10  $\mu\text{M}$  (9.26 kBq/mL) [ $^{14}\text{C}$ ]metformin. (B) HEK293 cells transfected with pBK-CMV vector (open circle), hOAT1 (open triangle), or hOAT3 (closed circle) were incubated for the specified periods at 37°C with 0.2 mL of 10  $\mu\text{M}$  (9.26 kBq/mL) [ $^{14}\text{C}$ ]metformin. Each point represents the mean  $\pm$  S.E. of three monolayers. (C-E) HEK293 cells transfected with pCMV6-XL4 vector (open column), hOCT1 (closed column) (C), hOCT2 (closed column) (D), or hOCT2-A (closed column) (E) were incubated at 37°C for 1 min with 0.2 mL of 5  $\mu\text{M}$  (10.36 kBq/mL) [ethyl-1- $^{14}\text{C}$ ]tetraethylammonium (TEA) bromide. (F) HEK293 cells transfected with pBK-CMV vector (open column), and hOAT1 (closed column) were incubated at 37°C for 1 min with 0.2 mL of 5  $\mu\text{M}$  (9.25 kBq/mL) *p*-[glycyl- $^{14}\text{C}$ ]aminohippuric acid (PAH). (G) HEK293 cells transfected with pBK-CMV vector (open column), and hOAT3 (closed column) were incubated at 37°C for 1 min with 0.2 mL of 20 nM (37 kBq/mL) [6,7- $^3\text{H}$ (*N*)]estrone sulfate (ES) ammonium salt. Each column represents the mean  $\pm$  S.E. of three monolayers.

Shimadzu Co.). The stationary phase was a Cosmosil 5C<sub>18</sub>-MS-II column (4.6-mm inside diameter  $\times$  150 mm, Nacalai Tesque, Kyoto Japan). The flow rate was 1 mL/min, and the column temperature was maintained at 40°C. The mobile phase consisted of 60% phosphate buffer (10 mM, pH 6.5) and 40% methanol.

**Analytical methods:** The plasma concentration at 0 min was extrapolated assuming that the concentration data could be fitted to the two-compartment model. The area under the plasma concentration-time curve until 3 min ( $\text{AUC}_{0-3\text{min}}$ ) was calculated by the trapezoidal rule. The tissue uptake clearance of metformin was calculated as dividing the tissue accumulation at 3 min by the  $\text{AUC}_{0-3\text{min}}$ .<sup>14)</sup>

**Statistical analysis:** Data are expressed as the mean  $\pm$  S.E. Data were analyzed statistically using a one-way analysis of variance (ANOVA) followed by Fisher's *t* test. Significance was set at  $P < 0.05$ .

## Results

**[ $^{14}\text{C}$ ]metformin by organic ion transporters:** First, we examined the [ $^{14}\text{C}$ ]metformin uptake by HEK293 cells transfected with hOCT1, hOCT2, hOCT2-A, hOAT1, and hOAT3 cDNAs. The uptake was markedly stimulated in the OCT2-transfected cells. On the other hand, much less [ $^{14}\text{C}$ ]metformin was taken up by

OCT1-transfected cells than OCT2-transfected cells. Other transfectants did not show an increase in the uptake of metformin (Figs. 1A and 1B). The functional expression of each transporter was confirmed using typical substrates (Figs. 1C-1G).

**Difference in metformin transport capacity between OCT1 and OCT2:** Next, we assessed whether the difference in the uptake of [ $^{14}\text{C}$ ]metformin via hOCT1 and hOCT2 was dependent on the expression level in the transfectants. After transfection with several amounts of hOCT1 or hOCT2 cDNA, each mRNA level (Fig. 2A) and metformin uptake (Fig. 2B) was evaluated. The metformin uptake by each hOCT1- or hOCT2-cDNA transfected HEK293 cells was saturated at the high mRNA level range. Figure 2C shows that the uptake of metformin by hOCT2 was much greater than that by hOCT1 at various mRNA levels. We recently reported that the apparent  $K_m$  and  $V_{\text{max}}$  values for the transport of metformin by HEK293 cells stably expressing hOCT2 were  $1.38 \pm 0.21$  mM and  $11.9 \pm 1.5$  nmol/mg protein/min, respectively.<sup>10)</sup> In the current study, we also established HEK293 cells stably expressing hOCT1. The apparent  $K_m$  and  $V_{\text{max}}$  values for the uptake of metformin by cells stably expressing hOCT1 were  $4.95 \pm 1.12$  mM and  $4.34 \pm 0.59$  nmol/mg protein/min, respectively. Because the hOCT1 and hOCT2

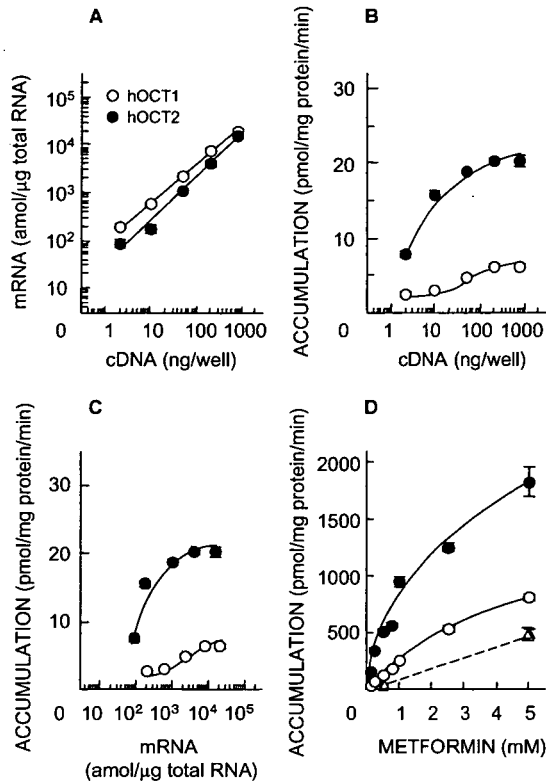


**Fig. 2.** Effects of mRNA expression levels of hOCT1 and hOCT2 on [<sup>14</sup>C]metformin transport.

(A) HEK293 cells cultured in 24-well plate were transfected into a well with 2, 10, 50, 200, and 800 ng of plasmid cDNA coding hOCT1 or hOCT2. The pCMV6-XL4 empty vector DNA was added to the DNA solution to give the final volume (800 ng/well) before transfection. Total cellular RNA was extracted from HEK293 cells transfected with several amounts of hOCT1 cDNA or hOCT2 cDNA. The mRNA levels of hOCT1 (open circle) and hOCT2 (closed circle) were determined by real-time PCR. Each point represents the mean  $\pm$  S.E. of three monolayers. (B) HEK293 cells transfected with several amounts of hOCT1 cDNA (open circle) or hOCT2 (closed circle) were incubated for 2 min at 37°C with 0.2 mL of 10  $\mu$ M (9.26 kBq/mL) [<sup>14</sup>C]metformin. Each point represents the mean  $\pm$  S.E. of three monolayers. (C) An illustration of the correlation between the mRNA level of hOCT1 or hOCT2 (A), and the accumulation of [<sup>14</sup>C]metformin (B). (D) HEK293 cells transfected with 50 ng/well of hOCT1 cDNA (open circle and open triangle) or hOCT2 (closed circle and closed triangle), and 750 ng/well of pCMV6-XL4 empty vector were incubated for 2 min at 37°C with 0.2 mL of 10  $\mu$ M (9.26 kBq/mL) [<sup>14</sup>C]metformin in the absence (circle) or presence (triangle) of 5 mM MPP (pH 7.4). Open and closed triangles are overlapping. Unlabeled metformin was added to [<sup>14</sup>C]metformin to give the final concentrations indicated. Each point represents the mean  $\pm$  S.E. of three monolayers.

mRNA were not detected in the cells transfected with the empty vector (data not shown), the present data were suggested to be derived by the transfected transporters.

**Kinetic evaluation of metformin transport by OCTs:** To establish more of a quantitative difference between hOCT1 and hOCT2 in the transport of metformin, we examined the concentration-dependence of [<sup>14</sup>C]met-

**Table 1.** Apparent  $K_m$  values of [<sup>14</sup>C]metformin uptake by human or rat OCT1 and OCT2.

|       | $K_m$<br>(mM)   | $V_{max}$<br>(pmol/mg protein/min) | Intrinsic clearance*<br>( $\mu$ L/min/fmol mRNA) |
|-------|-----------------|------------------------------------|--|
| hOCT1 | 1.47 $\pm$ 0.19 | 396 $\pm$ 42                       | 5.09 $\pm$ 0.52                                  |
| hOCT2 | 0.99 $\pm$ 0.03 | 1444 $\pm$ 81                      | 54.49 $\pm$ 4.64                                 |
| rOCT1 | 3.73 $\pm$ 0.15 | 145 $\pm$ 6                        | 0.39 $\pm$ 0.04                                  |
| rOCT2 | 0.63 $\pm$ 0.09 | 1446 $\pm$ 55                      | 36.98 $\pm$ 4.39                                 |

\*Values of intrinsic clearance were calculated as follows:  $V_{max}$  (pmol/mg protein)/ $K_m$  (mM)/mRNA expression level (amol/mg protein). Experimental conditions are in the legends of Fig. 2D and Fig. 3D. The apparent  $K_m$  and  $V_{max}$  values were determined from Eadie-Hofstee plots of metformin uptake after the corrections for nonsaturable components. Data are shown as means  $\pm$  S.E. of three monolayers.

formin uptake without saturating the mRNA expression levels using cells transfected with each OCT-cDNA (50 ng/well) and vector-cDNA (750 ng/well) (Fig. 2D). Table 1 shows the apparent  $K_m$  and  $V_{max}$  values for the uptake of metformin by hOCT1 and hOCT2. The clearance of metformin,  $V_{max}/K_m$ , was much higher in hOCT2-transfectants. Concerning the expression level of each transporter mRNA, the intrinsic clearance of the hOCT2-mediated uptake of metformin was about 10-fold that for the hOCT1-mediated uptake (Table 1). Prior to examining the tissue distribution of metformin in rats, we ascertained the correspondence between hOCTs and rOCTs. As shown in Fig. 3, the expression-level dependent manners of metformin transport by rOCT1 and rOCT2 was similar in comparison with those of human orthologue transporters. The apparent intrinsic clearance of rOCT2-mediated uptake of metformin was about 100-fold greater than rOCT1 (Table 1). To confirm the transport activity of these OCTs, we also examined the similar experiments using TEA as a reference substrate (Fig. 4). The expression-level dependent manners of TEA uptakes by OCTs were observed. Although hOCT2-mediated uptake of TEA was tended to be similar with hOCT1 (Fig. 4A), rOCT2-mediated TEA uptake was much greater than rOCT1 (Fig. 4B).

To estimate the tissue intrinsic clearance of metformin in the liver or kidney focusing on the organic cation transporters, we quantified the mRNA expression amounts of rOCT1 and rOCT2 in the whole liver (12.3  $\pm$  0.3 g/rat, mean  $\pm$  S.E. of four rats) and kidney (2.1  $\pm$  0.03 g/rat, mean  $\pm$  S.E. of four rats) of rats. As shown in the Fig. 5, the mRNA expression level of rOCT2 in the kidneys was 10.3 and 6.5 fold higher in comparison with the renal rOCT1 and the hepatic rOCT1, respectively. Next, the tissue intrinsic clearance of rOCT-mediated uptake of metformin in each tissue per rat was estimated in combination with the data in Table 1. The renal intrinsic clearance of rOCT2-mediated uptake of

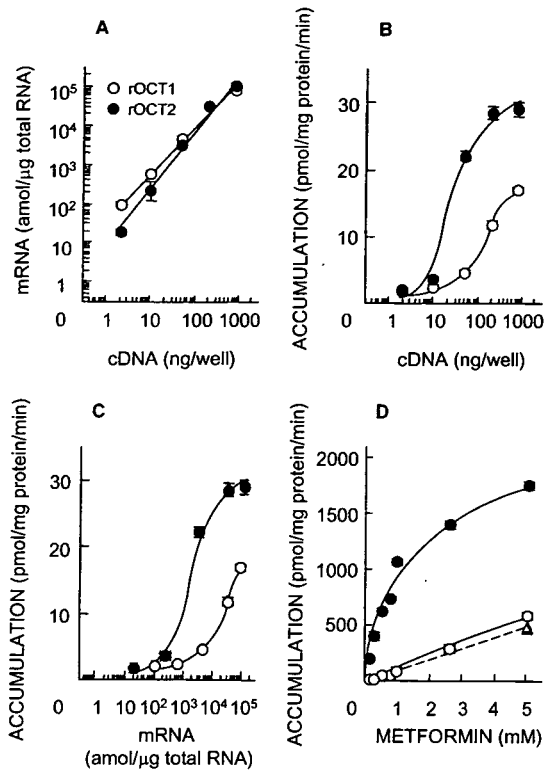


Fig. 3. Effects of expression levels of rOCT1 and rOCT2 on [<sup>14</sup>C]metformin transport.

The experimental conditions were correspondingly conducted to those of Fig. 2. HEK293 cells were transfected with the several amounts of plasmid cDNA coding rOCT1 or rOCT2, and pBK-CMV empty vector DNA instead of hOCT1 or hOCT2, and pCMV6-XL4 empty vector, respectively.

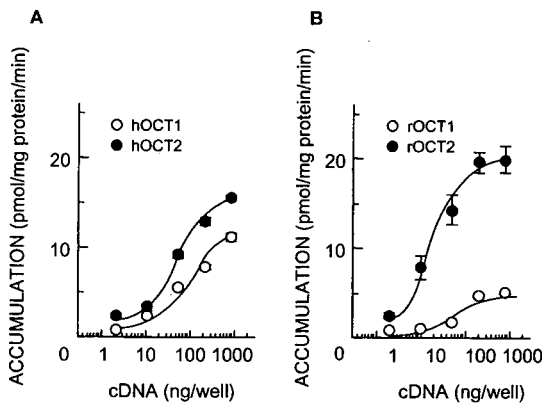


Fig. 4. Effects of expression levels of organic cation transporters on [<sup>14</sup>C]TEA transport.

The experimental conditions were correspondingly conducted as described for Fig. 2B. HEK293 cells were transfected with the several amounts of plasmid cDNA coding hOCT1 (open circle, A), hOCT2 (closed circle, A), pCMV6-XL4 empty vector DNA (A), rOCT1 (open circle, B) or rOCT2 (closed circle, B), and pBK-CMV empty vector DNA (B).

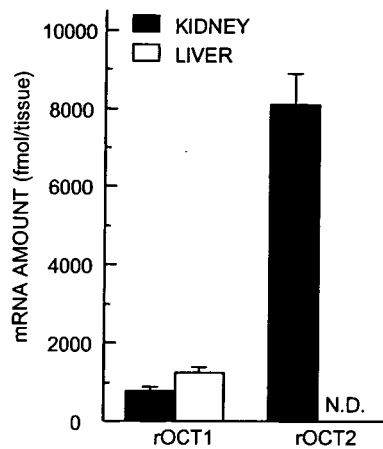


Fig. 5. mRNA expression levels of rOCT1 and rOCT2 in whole liver and kidney.

After harvesting the whole liver and kidneys from the male rats (12 weeks, 300-330 weighing), total RNA was extracted as described in the method section. The mRNA levels of rOCT1 and rOCT2 in the each tissue were determined by real-time PCR. The wet weights of liver and kidneys were  $12.3 \pm 0.3$  and  $2.1 \pm 0.03$  g/rat (mean  $\pm$  S.E. of four rats), respectively. Each point represents the mean  $\pm$  S.E. of four rats. N.D., not detected.

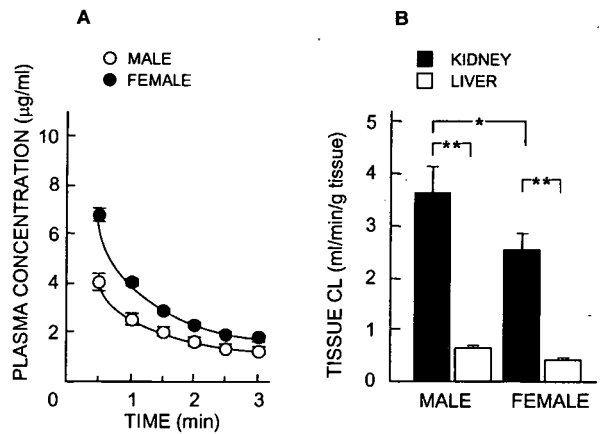


Fig. 6. Plasma concentration curves (A) and tissue uptake clearance (B) of metformin in rats.

Metformin (1 mg/kg) was administered as a bolus *via* the right femoral vein of male (open circle) or female (closed circle) rats. (A) Blood samples were collected from the left femoral artery at 0.5, 1, 1.5, 2, 2.5, and 3 min after the injection. Each point represents the mean  $\pm$  S.E. of five rats. (B) Three minutes after the administration of metformin, the tissues were harvested. The concentration of metformin in each tissue was measured. The tissue uptake clearance of metformin was calculated as dividing the tissue accumulation at 3 min by the AUC<sub>0-3min</sub> from each rat. The wet weights of liver and kidneys in male rats were  $8.5 \pm 0.3$  and  $1.94 \pm 0.05$  g/rat, and those in female rats were  $7.9 \pm 0.3$  and  $1.5 \pm 0.04$  g/rat, respectively (mean  $\pm$  S.E. of five rats). Each column represents the mean  $\pm$  S.E. for five rats. \* $p < 0.05$ , \*\* $p < 0.01$ , significant differences.

metformin was 299.8 mL/min/tissue, which was markedly higher than that by renal rOCT1 (0.31 mL/min/tissue) and hepatic rOCT1 (0.49 mL/min/tissue). The contribution of rOCT1 on the renal distribution of metformin was negligible compared to rOCT2.

***In vivo* pharmacokinetic role of rOCT1 and rOCT2 on metformin tissue distribution:** Furthermore, we examined the tissue distribution of metformin *in vivo* focusing on rOCT1 and rOCT2. We previously reported that the levels of rOCT2 mRNA and protein in the kidney were much higher in males than females, but there was no gender-based difference in the mRNA expression of renal rOCT1.<sup>15)</sup> Considering these findings, we examined the contribution of rOCT2 to the tissue distribution of metformin using male and female rats. The plasma concentrations of metformin until 3 min after the intravenous administration and the tissue uptake clearances of metformin were determined (Fig. 6). The tissue uptake clearance of metformin in the male kidney was much higher than that in male liver, female liver, and female kidney.

### Discussion

In the present study, we have quantitatively elucidated the substrate specificity of OCTs. hOCT2 was identified as a superior transporter mediating the uptake of metformin among several human organic ion transporters examined (Fig. 1), and two transporters, OCT1 and OCT2, had distinct substrate affinity for metformin (Figs. 2 and 3). Although the expression-level dependent profile of TEA uptake by hOCT1 and hOCT2 was similar, the TEA uptake activity of rOCT2 was much greater in comparison with rOCT1 (Fig. 4). By analysing the relation between the expression level and transport activity, some differences on the transport characteristics between rOCT1 and rOCT2 would be clarified. It had been considered that OCT1 and OCT2 possess similar multispecificities for various compounds.<sup>5,16-18)</sup> However, recent reports suggest that some chemical compounds such as guanidine and creatinine could be used to determine the molecular selectivity between OCT1 and OCT2.<sup>11,19)</sup> In addition, hOCT2-A, a splicing variant of hOCT2, did not transport metformin (Fig. 1A). Therefore, metformin may be an useful probe substrate for clarifying the structural determinant(s) to distinguish the substrate specificities between hOCT2 and hOCT2-A. By use of the transfectants with a limit amount of cDNA, we have simultaneously demonstrated that metformin, which is a derivative of guanidine, was dominantly transported by OCT2 compared to OCT1. To our knowledge, this is the first report demonstrating the quantitative difference in the transport activities of metformin between OCT1 and OCT2. Information about the molecular determinants of substrate binding has emerged gradually.<sup>20)</sup>

The use of guanidine derivatives including metformin, will clarify the chemical structures required for specific transport by OCT2.

In rat kidney, rOCT2 expression levels were higher in male than female rats, and the uptake of TEA in the renal slices was greater in the male rats.<sup>15)</sup> In the present study, the renal uptake clearance of metformin was also higher in male than female rats, comparable with previous findings. In the male rats, the mRNA expression level of rOCT2 in the kidneys was markedly higher than the hepatic rOCT1 (Fig. 5), and the estimated renal intrinsic clearance of metformin by rOCT2 was about 600 times larger than that of the liver by rOCT1. The *in vivo* tissue uptake clearance of metformin in the male kidney was about 6 times larger than that in the male liver (Fig. 6), and therefore, the plasma flow rate in the kidney might be a limiting factor for metformin renal distribution. Considering the expression levels and the intrinsic clearance of transporter-mediated metformin uptake, there is little contribution of rOCT1 on renal uptake of metformin. Because the hOCT1 was not detected in the human kidney, the hOCT2 was considered as a primary organic cation transporter determining the renal distribution of cationic drugs.<sup>4)</sup> These results indicate that rat is still useful model animal for pharmacokinetic studies of metformin focusing on the hepatic rOCT1 and renal rOCT2. This is the first report to estimate the expressional amounts of organic cation transporter isoforms in the whole liver and kidneys, and these data will be useful to quantitative evaluation of the tissue selectivity of cationic drugs in rodents.

In the present study, the accumulation of metformin in the liver was much lower than that in the kidney (Fig. 6). Because the plasma flow rate could be a limited step, the difference between metformin accumulation into the kidneys and livers was small compared to the *in vitro* estimation (Table 1, Figs. 5 and 6). However, the expressional dominance of the rOCT2 in male kidney reflected the concentrated accumulation of metformin in comparison with that in the female rats. Therefore, the expressional amount as well as substrate specificity of transporters in each tissue was suggested to help understanding the tissue selectivity of cationic drugs. In the humans, the kidney function as well as the age was postulated as the predictors for pharmacokinetics of metformin.<sup>6)</sup> Although the OCT1 protein is expressed in the kidney and liver in the rat, the expression of OCT1 in the human kidney is negligible.<sup>4,5)</sup> Therefore, considering the present *in vitro* and *in vivo* results, it was suggested that renal OCT2 should be more important for the pharmacokinetics of metformin in comparison with hepatic OCT1.

The mechanisms behind the pharmacological actions of metformin have been described, including decreased hepatic glucose production and increased glycogenesis

and lactate production. The liver had been generally considered to be the primary glucogenic organ, except in acidotic conditions. But several studies have provided considerable evidence that mammalian kidney can make glucose and release it under various conditions.<sup>21)</sup> Since 1938, it has been said that animals' kidney is also a producer of glucose.<sup>22,23)</sup> Stumvoll *et al.*<sup>24)</sup> suggested an important role for the human kidney in glucose homeostasis, using the combined isotopic-net renal balance approach. Furthermore, the role of the kidney in gluconeogenesis during diabetes has been studied.<sup>21)</sup> In the present study, the concentrative accumulation of metformin in the kidney by OCT2 has been revealed. These backgrounds, including the present results, suggest that the pharmacological effects of metformin in the kidney as well as liver may be important. Clinical studies of biguanides in diabetic patients should be performed to clarify the pharmacodynamic as well as pharmacokinetic significance of renal OCT2 for the control of blood glucose levels.

In conclusion, the quantitative difference in the metformin transport between OCT1 and OCT2 has been firstly clarified using the limited amount of transfected cDNA, and it has been suggested that the renal OCT2 plays a dominant role for metformin pharmacokinetics.

### References

- 1) Gründemann, D., Gorboulev, V., Gambaryan, S., Veyhl, M. and Koepsell, H.: Drug excretion mediated by a new prototype of polyspecific transporter. *Nature*, **372**: 549–552 (1994).
- 2) Okuda, M., Saito, H., Urakami, Y., Takano, M. and Inui, K.: cDNA cloning and functional expression of a novel rat kidney organic cation transporter, OCT2. *Biochem. Biophys. Res. Commun.*, **224**: 500–507 (1996).
- 3) Gorboulev, V., Ulzheimer, J. C., Akhoundova, A., Ulzheimer-Teuber, I., Karbach, U., Quester, S., Baumann, C., Lang, F., Busch, A. E. and Koepsell, H.: Cloning and characterization of two human polyspecific organic cation transporters. *DNA Cell Biol.*, **16**: 871–881 (1997).
- 4) Motohashi, H., Sakurai, Y., Saito, H., Masuda, S., Urakami, Y., Goto, M., Fukatsu, A., Ogawa, O. and Inui, K.: Gene expression levels and immunolocalization of organic ion transporters in the human kidney. *J. Am. Soc. Nephrol.*, **13**: 866–874 (2002).
- 5) Inui, K., Masuda, S. and Saito H.: Cellular and molecular aspects of drug transport in the kidney. *Kidney Int.*, **58**: 944–958 (2000).
- 6) Sambol, N. C., Chiang, J., Lin, E. T., Goodman, A. M., Liu, C. Y., Benet, L. Z. and Cogan, M. G.: Kidney function and age are both predictors of pharmacokinetics of metformin. *J. Clin. Pharmacol.*, **35**: 1094–1102 (1995).
- 7) Wang, D. S., Jonker, J. W., Kato, Y., Kusuhara, H., Schinkel, A. H. and Sugiyama, Y.: Involvement of organic cation transporter 1 in hepatic and intestinal distribution of metformin. *J. Pharmacol. Exp. Ther.*, **302**: 510–515 (2002).
- 8) Wang, D. S., Kusuhara, H., Kato, Y., Jonker, J. W., Schinkel, A. H. and Sugiyama, Y.: Involvement of organic cation transporter 1 in the lactic acidosis caused by metformin. *Mol. Pharmacol.*, **63**: 844–848 (2003).
- 9) Dresser, M. J., Xiao, G., Leabman, M. K., Gray, A. T. and Giacomini, K. M.: Interactions of n-tetraalkylammonium compounds and biguanides with a human renal organic cation transporter (hOCT2). *Pharm. Res.*, **19**: 1244–1247 (2002).
- 10) Kimura, N., Okuda, M. and Inui, K.: Metformin transport by renal basolateral organic cation transporter hOCT2. *Pharm. Res.*, **22**: 255–259 (2005).
- 11) Urakami, Y., Kimura, N., Okuda, M. and Inui, K.: Creatinine transport by basolateral organic cation transporter hOCT2 in the human kidney. *Pharm. Res.*, **21**: 976–981 (2004).
- 12) Urakami, Y., Akazawa, M., Saito, H., Okuda, M. and Inui, K.: cDNA cloning, functional characterization, and tissue distribution of an alternatively spliced variant of organic cation transporter hOCT2 predominantly expressed in the human kidney. *J. Am. Soc. Nephrol.*, **13**: 1703–1710 (2002).
- 13) Bradford, M. M.: A Rapid and sensitive method for the quantitation of microgram quantities of protein utilizing the principle of protein-dye binding. *Anal. Biochem.*, **72**: 248–254 (1976).
- 14) Ji, L., Masuda, S., Saito, H. and Inui, K.: Down-regulation of rat organic cation transporter rOCT2 by 5/6 nephrectomy. *Kidney Int.*, **62**: 514–524 (2002).
- 15) Urakami, Y., Nakamura, N., Takahashi, K., Okuda, M., Saito, H., Hashimoto, Y. and Inui, K.: Gender differences in expression of organic cation transporter OCT2 in rat kidney. *FEBS Lett.*, **461**: 339–342 (1999).
- 16) Urakami, Y., Okuda, M., Masuda, S., Saito, H. and Inui, K.: Functional characteristics and membrane localization of rat multispecific organic cation transporters, OCT1 and OCT2, mediating tubular secretion of cationic drugs. *J. Pharmacol. Exp. Ther.*, **287**: 800–805 (1998).
- 17) Okuda, M., Urakami, Y., Saito, H. and Inui, K.: Molecular mechanisms of organic cation transport in OCT2-expressing *Xenopus* oocytes. *Biochim. Biophys. Acta.*, **1417**: 224–231 (1999).
- 18) Urakami, Y., Okuda, M., Masuda, S., Akazawa, M., Saito, H. and Inui, K.: Distinct characteristics of organic cation transporters, OCT1 and OCT2, in the basolateral membrane of renal tubules. *Pharm. Res.*, **18**: 1528–1534 (2001).
- 19) Gründemann, D., Liebich, G., Kiefer, N., Koster, S. and Schomig, E.: Selective substrates for non-neuronal monoamine transporters. *Mol. Pharmacol.* **56**: 1–10 (1999).
- 20) Gorboulev, V., Shatskaya, N., Volk, C. and Koepsell, H.: Subtype-specific affinity for corticosterone of rat organic cation transporters rOCT1 and rOCT2 depends on three amino acids within the substrate binding region. *Mol. Pharmacol.*, **67**: 1612–1619 (2005).

- 21) Gerich, J. E., Meyer, C., Woerle, H. J. and Stumvoll, M.: Renal gluconeogenesis: its importance in human glucose homeostasis. *Diabetes Care.*, **24**: 382-391 (2001).
- 22) Bergman, H. and Drury, D. R.: The relationship of kidney function to the glucose utilization of the extra abdominal tissues. *Am. J. Physiol.*, **124**: 279-284 (1938).
- 23) Reinecke, R.: The kidney as a source of glucose in the eviscerated rat. *Am. J. Physiol.*, **140**: 276-285 (1943).
- 24) Stumvoll, M., Chintalapudi, U., Perriello, G., Welle, S., Gutierrez, O. and Gerich, J.: Uptake and release of glucose by the human kidney. Postabsorptive rates and responses to epinephrine. *J. Clin. Invest.*, **96**: 2528-2533 (1995).



## Short Communication

### MODULATION OF P-GLYCOPROTEIN EXPRESSION IN HYPERTHYROID RAT TISSUES

Received March 19, 2005; accepted August 3, 2005

#### ABSTRACT:

P-glycoprotein (Pgp) is expressed in various normal tissues and plays an important role in drug absorption and disposition. In addition, it is supposed that alterations in the expression levels of Pgp are involved in the inter- and intraindividual variability of pharmacokinetics of many drugs. Since pharmacokinetic properties of various drugs are altered in patients with thyroid disorders, we examined the expression of Pgp and *mdr1a/1b* mRNA in the kidney, liver, jejunum, and ileum from euthyroid and hyperthyroid rats. Western blot analysis revealed that Pgp expression was markedly increased in the kidney and liver of hyperthyroid rats. In contrast,

it was slightly increased in the jejunum and ileum. *mdr1a/1b* mRNA levels were significantly increased in the kidney of hyperthyroid rats. However, they were not increased in the liver as well as in the jejunum and ileum of hyperthyroid rats. Expression levels of bile salt export pump and *mdr2* mRNA were also unchanged in hyperthyroid rat liver. Taken together, these findings suggest that thyroid hormone induces Pgp expression in a tissue-selective manner, and that the modulation of *mdr1a/1b* mRNA expression in the hyperthyroid state varies among tissues.

P-glycoprotein (Pgp) is expressed in various tissues such as brain, liver, kidney, and intestine (Cordon-Cardo et al., 1990; Brady et al., 2002) and plays an important role in defining the pharmacokinetics of many drugs. Pgp functions as a drug efflux pump and exports hydrophobic, bulky drugs such as anticancer agents, cardiac glycosides,  $\beta$ -blockers, calcium channel blockers, and immunosuppressants. Since Pgp has a broad substrate recognition, the concomitant administration of drugs often causes drug interactions by inhibiting Pgp-mediated transport (Yu, 1999). For example, inhibition of digoxin transport in cultured epithelial cell lines expressing Pgp by various drugs such as quinidine (Tanigawara et al., 1992; Fromm et al., 1999), verapamil (Tanigawara et al., 1992), and cyclosporin A (Okamura et al., 1993) has been reported. We have also demonstrated that the renal clearance of digoxin was decreased in patients receiving a concomitant administration of clarithromycin and, accordingly, the plasma concentration of digoxin was increased (Wakasugi et al., 1998). The mechanism of this interaction was explained by the inhibition of Pgp-mediated tubular secretion of digoxin. On the other hand, recent studies have demonstrated that changes in the expression levels of Pgp affect the pharmacokinetic properties of Pgp substrates. Greiner et al. (1999) reported that rifampin administration induced Pgp expression in the small intestine and reduced the plasma concentration of orally administered digoxin, suggesting that alterations in the expression levels of Pgp are closely involved in the inter- and intraindividual variability of pharmacokinetics of Pgp substrates.

Thyroid hormone is secreted from the thyroid gland to maintain

This work was supported in part by 21st Century COE Program "Knowledge Information Infrastructure for Genome Science," by a Grant-in-Aid for Scientific Research from the Ministry of Education, Culture, Sports, Science and Technology of Japan, and by The Nakatomi Foundation. N.N. is supported as a Teaching Assistant by 21st Century Center of Excellence (COE) Program "Knowledge Information Infrastructure for Genome Science."

Article, publication date, and citation information can be found at <http://dmd.aspetjournals.org>.

doi:10.1124/dmd.105.004770.

normal growth and development, normal body temperature, and normal energy levels. Most of its effects appear to be mediated by the activation of nuclear receptors that lead to increased expression of mRNA and subsequent protein synthesis. Disorders of the thyroid gland are among the most common endocrine disorders, and are known as hyperthyroidism and hypothyroidism. It was reported that pharmacokinetic properties of various drugs were altered in patients with thyroid disorders (Shenfield, 1981; O'Connor and Feely, 1987). As for Pgp substrates, plasma concentrations of digoxin were decreased in patients with hyperthyroidism as compared with euthyroid patients. Such an altered pharmacokinetics of digoxin in hyperthyroid patients has been explained by an increase in renal clearance (Lawrence et al., 1977) and volume of distribution (Shenfield et al., 1977; Shenfield, 1981). The reason for the increased renal clearance of digoxin is considered to be a facilitation of tubular secretion (Bonelli et al., 1978); however, the mechanisms underlying the altered pharmacokinetics of digoxin in thyroid disease have not been fully elucidated.

Previous studies have shown that thyroid hormone regulates the expression levels of various membrane transporters such as the fructose transporter GLUT5 (Matosin-Matekalo et al., 1999), the peptide transporter PEPT1 (Ashida et al., 2002),  $\text{Na}^+/\text{K}^+$ -ATPase (Giannella et al., 1993), and the  $\text{Na}^+/\text{H}^+$  exchanger NHE1 (Li et al., 2002). Therefore, we hypothesized that the alteration in the plasma concentration of digoxin in patients with thyroid disorders might be due to changes in Pgp expression by thyroid hormone. In the present study, to elucidate the influence of a hyperthyroid state on the expression of Pgp in various tissues, we investigated Pgp and *mdr1a/1b* mRNA levels in liver, kidney, jejunum, and ileum from euthyroid and hyperthyroid rats.

#### Materials and Methods

**Materials.** L-Thyroxine ( $\text{T}_4$ ) was purchased from Sigma-Aldrich (St. Louis, MO). Monoclonal antibody C219 and anti-villin polyclonal antibody were obtained from CIS Bio International (Gif-sur-Yvette, France) and Santa Cruz

**ABBREVIATIONS:** Pgp, P-glycoprotein;  $\text{T}_4$ , L-thyroxine; bsep, bile salt export pump; PCR, polymerase chain reaction.

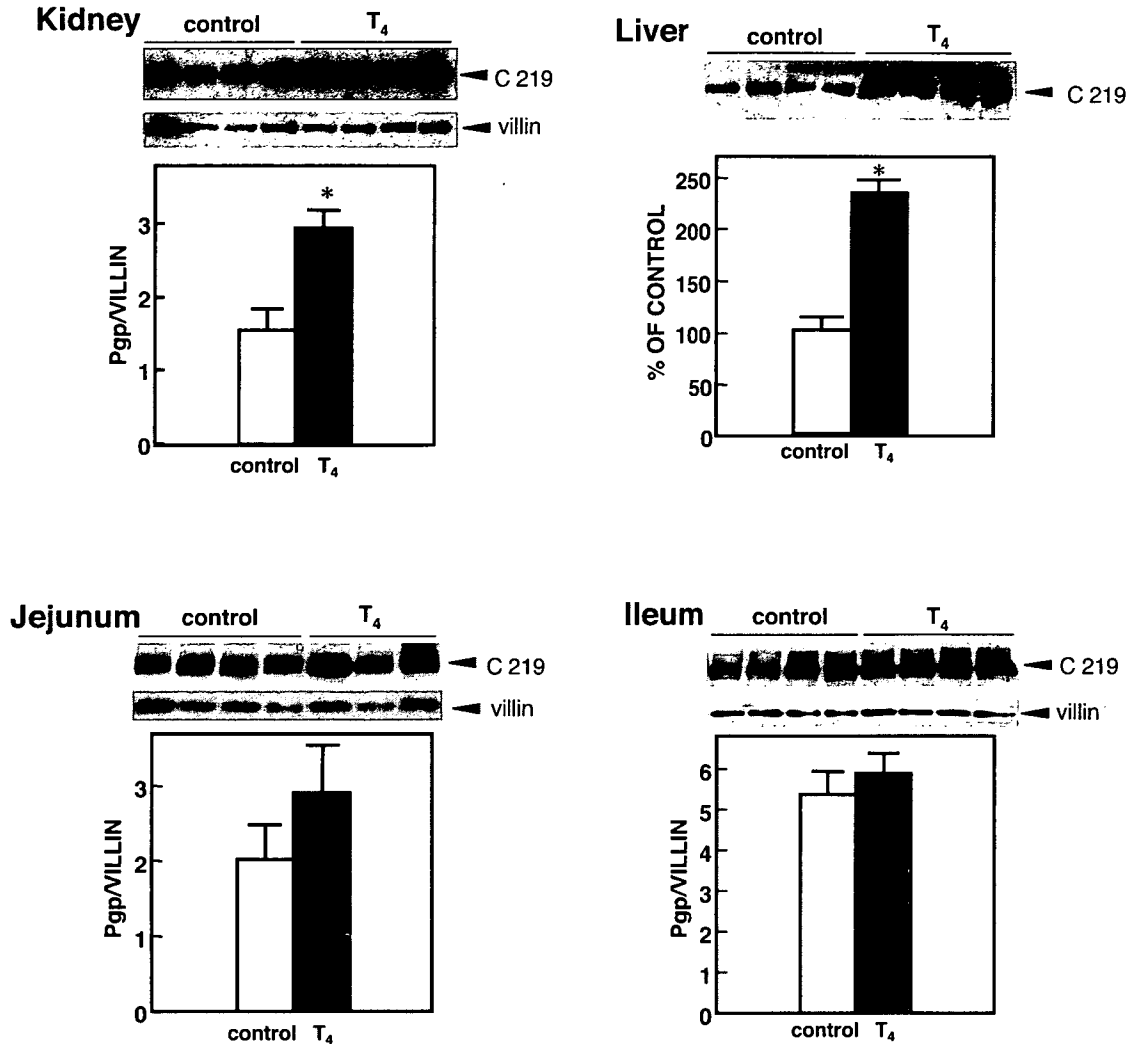


FIG. 1. Western blot analysis of the crude membranes from rat tissues for Pgp. Upper panel, immunoblotting of crude membranes from kidney, liver, jejunum, and ileum of hyperthyroid rats ( $T_4$ ) or euthyroid rats (control). Lower panel, densitometric quantification of Pgp. Each column represents the mean  $\pm$  S.E. of 3~7 rats. \*,  $p < 0.05$ , significantly different from control.

Biotechnology, Inc. (Santa Cruz, CA), respectively. All other chemicals used were of the highest purity available.

**Animals.** The animal experiments were performed in accordance with the Guideline for Animal Experiments of Kyoto University. Eight-week-old male Wistar rats were housed in a temperature- and humidity-controlled room and fed rat chow ad libitum. Hyperthyroidism was induced by adding  $T_4$  (12 mg/l) to the drinking water for 21 days as previously described (Ashida et al., 2004). After treatment, the kidney, liver, jejunum, and ileum were excised. Blood was also collected for measurement of plasma level of  $T_3$ . Plasma  $T_3$  levels in euthyroid and hyperthyroid rats were measured by an Enzyme Immuno Assay method (IMx; Dainabot, Tokyo, Japan). Plasma  $T_3$  levels in euthyroid and hyperthyroid rats were  $0.32 \pm 0.02$  and  $2.40 \pm 0.18$  ng/ml, respectively (mean  $\pm$  S.E.,  $n = 6$ ). In addition, hyperthyroid rats lost an average of 0.055 kg in response to  $T_4$  treatment (data not shown).

**Western Blot Analysis.** Isolation of crude plasma membrane fractions from each tissue and Western blot analysis were performed as described previously (Ogihara et al., 1996). Monoclonal antibody C219 and anti-villin polyclonal antibody were used as primary antibodies.

**RNA Isolation, Semiquantitative Reverse Transcription-Polymerase Chain Reaction (PCR), and Competitive PCR.** RNA isolation, reverse transcription, and competitive PCR procedures were performed as described previously (Masuda et al., 2000) with some modifications. The specific primer sets (5  $\mu$ M) used were as follows: for rat *mdr1a* primers, 5'-GATGGAATT-GATAATGTGGACA-3' and 5'-AAGGATCAGGAACAATAAAA-3'; for rat *mdr1b* primers, 5'-GAAATAATGCTTATGAATCCCAAA G-3' and 5'-

GGTTTCATGGTCGTCGTCCTTGA-3' (Zhang et al., 1996); for rat bile salt export pump (bsep) primers, 5'-GAGGTTACTTAATAGCCTACG-3' and 5'-CATCTATCATCACAGTTCCTCC-3'; and for rat *mdr2* primers, 5'-AA-GAATTTGAAGTTGAGCTAAGTGA-3' and 5'-TGGTTTCCACATCCAGC CTAT-3'. For the detection of *mdr1a* and *mdr1b*, semilogarithmic serial dilutions of mimic competitor DNA from 50 to 0.01 amol were added.

**Statistical Analysis.** Data were analyzed statistically using the nonpaired *t* test. Probability values of less than 5% were considered significant.

## Results and Discussion

To investigate the effect of thyroid hormone on the expression of Pgp, we examined the Pgp expression by Western blotting. As shown in Fig. 1, the expression of Pgp was remarkably increased in crude membranes of hyperthyroid rat kidney and liver (1.9-fold and 2.3-fold, respectively) as compared with those of euthyroid rats. In contrast, hyperthyroidism caused a slight increase in the expression of Pgp in rat jejunum and ileum (1.1-fold and 1.4-fold, respectively). These results suggest that the differences in the behavior of thyroid hormone in each tissue are involved in tissue selectivity of Pgp induction. Similarly, it was reported that MDR1 mRNA was elevated in a dexamethasone-treated human hepatoma cell line but not in a nonhepatoma cell line, suggesting that the hormonal regulation of *mdr* gene expression is gene- and cell type-specific (Zhao et al., 1993).

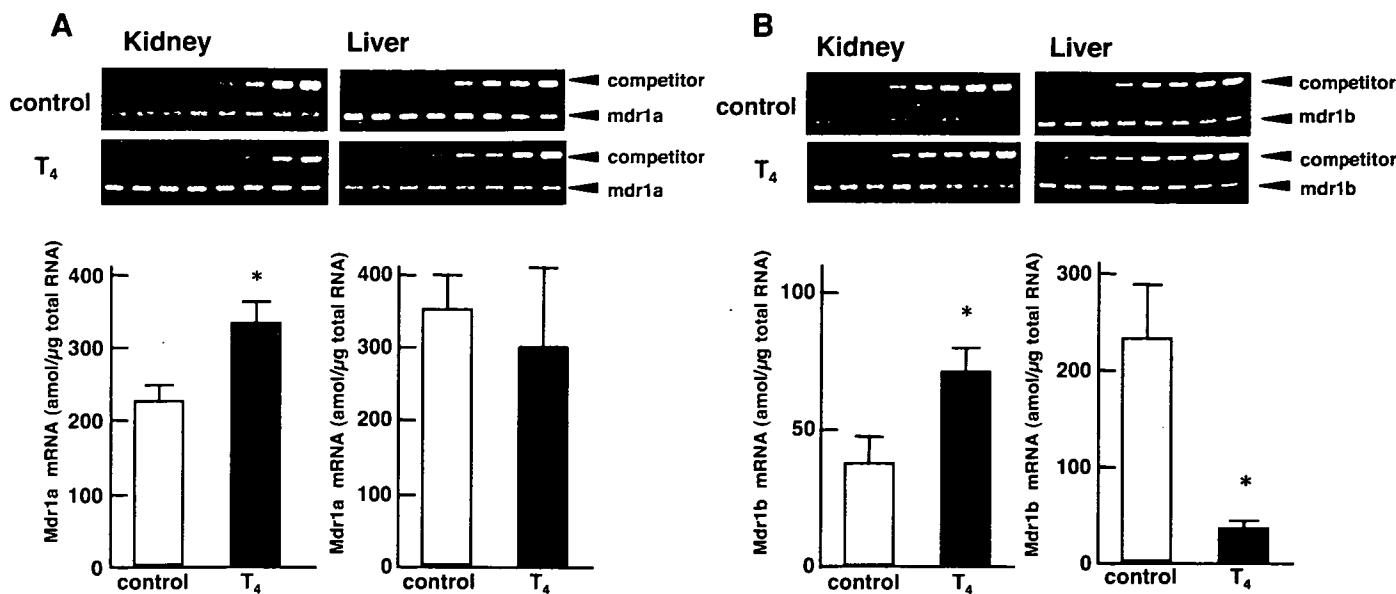


FIG. 2. Effect of hyperthyroidism on the expression of mdr1a (A) and mdr1b (B) mRNA in rat kidney and liver. Upper panel, typical results of agarose gel electrophoresis of the PCR products from each tissue of hyperthyroid rats (T<sub>4</sub>) or euthyroid rats (control). Eight points were selected with serial dilutions of mdr1a/1b mimic competitor cDNA from 0.01 to 25 amol. Lower panel, densitometric quantification of mdr1a and mdr1b mRNA. Each column represents the mean  $\pm$  S.E. of four rats. \*,  $p < 0.05$ , significantly different from control.

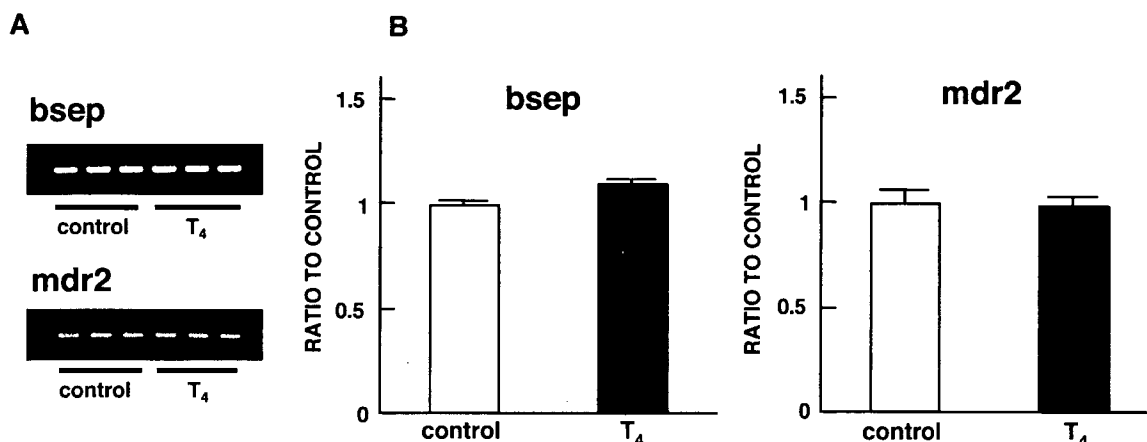


FIG. 3. Effect of hyperthyroidism on the expression of bsep and mdr2 mRNA in rat liver. A, typical results of agarose gel electrophoresis of the PCR products from liver of hyperthyroid rats (T<sub>4</sub>) or euthyroid rats (control). B, densitometric quantification of bsep and mdr2 mRNA. Each column represents the mean  $\pm$  S.E. of three rats.

Their report supports our results suggesting that the regulation of Pgp expression by thyroid hormone was possibly tissue-specific.

We then examined the expression of mdr1a and mdr1b mRNA using competitive PCR in each tissue. As shown in Fig. 2, the expression of both mdr1a and mdr1b mRNA was significantly increased in hyperthyroid rat kidney as compared with the control. Since the action of thyroid hormone appears to be mediated by the activation of nuclear receptors, which leads to increased levels of mRNA and subsequent protein synthesis (Ribeiro et al., 1995), it is likely that the induction of Pgp expression in the hyperthyroid kidney is mediated by the increased transcription of mdr1a/1b mRNA. On the other hand, hyperthyroidism caused a significant decrease in the expression of mdr1b mRNA in the liver but did not affect the expression of mdr1a mRNA. Since it was reported that C219 antibody reacted with not only Pgp but bsep and mdr2 (Childs et al., 1995) and bsep and mdr2 are expressed in the liver, we examined whether the immunoreactive protein bands obtained using C219 antibody reflected the induction of these transporters in hyperthyroid liver. As shown in Fig. 3, however, the expression of bsep and mdr2 mRNA did not change in hyperthy-

roid rat liver. Although the precise mechanism is not clear at this stage, thyroid hormone may regulate Pgp expression via nontranscriptional control in the liver. Further studies are needed to elucidate the regulation of Pgp and MDR1 by thyroid hormone in the liver.

Siegmund et al. (2002) examined the effect of levothyroxine administration on human intestinal Pgp expression. They demonstrated that duodenal MDR1 mRNA expression and immunoreactive Pgp were increased by levothyroxine administration, although the increase in MDR1 mRNA was not significant. However, changes in the expression of Pgp were not associated with major alterations in the pharmacokinetics of talinolol, a substrate of Pgp. In addition, the effect of thyroid hormone on the expression of Pgp in other tissues was not elucidated. In the present study, we observed a significant increase in Pgp expression in the kidney and liver (Fig. 2) and a slight increase in the intestine (Fig. 4) in hyperthyroid rats. Our results suggest that the decrease in the serum concentration of digoxin in hyperthyroidism is attributable to the increased expression of Pgp in the kidney and/or liver. Further studies are needed to assess the pharmacokinetics of Pgp substrates in hyperthyroid rats.

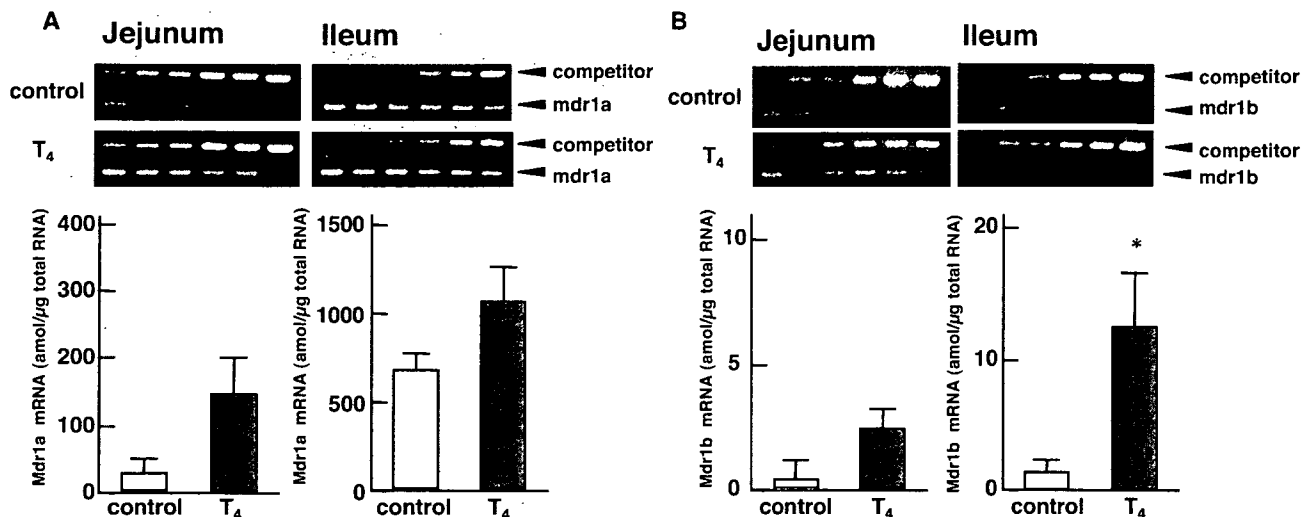


Fig. 4. Effect of hyperthyroidism on the expression of mdr1a (A) and mdr1b (B) mRNA in rat jejunum and ileum. Upper panel, typical results of agarose gel electrophoresis of the PCR products from each tissue of hyperthyroid rats (T<sub>4</sub>) or euthyroid rats (control). Six points were selected with serial dilutions of mdr1a/1b mimic competitor cDNA from 0.25 to 50 amol. Lower panel, densitometric quantification of mdr1a and mdr1b mRNA. Each column represents the mean  $\pm$  S.E. of four rats. \*,  $p < 0.05$ , significantly different from control.

For obvious ethical reasons, Siegmund et al. (2002) administered levothyroxine in doses that do not cause thyrotoxicosis. In the present study, the expression of Pgp was only slightly increased in rat intestinal tissues, although we used hyperthyroid rats. It is known that the gene encoding Pgp differs between humans and rats. Pgp is encoded by *MDR1* in humans and by *mdr1a* and *mdr1b* in rats. Therefore, it is supposed that the mechanisms by which thyroid hormone induces Pgp expression differ between species, and Pgp expression in human intestinal tissues may increase dramatically under thyrotoxicosis.

In conclusion, thyroid hormone induces Pgp expression in a tissue-selective manner. In addition, the modulation of mdr1a/1b mRNA expression in the hyperthyroid state varied among tissues. These results provide useful information for elucidating the drug interaction and pharmacokinetic variability in thyrotoxicosis.

Department of Pharmacy,  
Kyoto University Hospital,  
Faculty of Medicine,  
Kyoto University,  
Sakyo-ku, Kyoto, Japan

NAOKI NISHIO  
TOSHIYA KATSURA  
KAYOKO ASHIDA  
MASAHIRO OKUDA  
KEN-ICHI INUI

#### References

- Ashida K, Katsura T, Motohashi H, Saito H, and Inui K (2002) Thyroid hormone regulates the activity and expression of the peptide transporter PEPT1 in Caco-2 cells. *Am J Physiol* 282:G617–G623.
- Ashida K, Katsura T, Saito H, and Inui K (2004) Decreased activity and expression of intestinal oligopeptide transporter PEPT1 in rats with hyperthyroidism *in vivo*. *Pharm Res (NY)* 21: 969–975.
- Bonelli J, Haydl H, Hrudy K, and Kaik G (1978) The pharmacokinetics of digoxin in patients with manifest hyperthyroidism and after normalization of thyroid function. *Int J Clin Pharmacol Biopharm* 16:302–306.
- Brady JM, Cherrington NJ, Hartley DP, Buist SC, Li N, and Klaassen CD (2002) Tissue distribution and chemical induction of multiple drug resistance genes in rats. *Drug Metab Dispos* 30:838–844.
- Childs S, Yeh RL, Georges E, and Ling V (1995) Identification of sister gene to P-glycoprotein. *Cancer Res* 55:2029–2034.
- Cordon-Cardo C, O'Brien JP, Boccia J, Casals D, Bertino JR, and Melamed MR (1990) Expression of the multidrug resistance gene product (P-glycoprotein) in human normal and tumor tissues. *J Histochem Cytochem* 38:1277–1287.
- Fromm MF, Kim RB, Stein CM, Wilkinson GR, and Roden DM (1999) Inhibition of P-glycoprotein-mediated drug transport: A unifying mechanism to explain the interaction between digoxin and quinidine. *Circulation* 99:552–557.
- Giannella RA, Orłowski J, Jump ML, and Lingrel JB (1993) Na<sup>+</sup>-K<sup>+</sup>-ATPase gene expression in rat intestine and Caco-2 cells: response to thyroid hormone. *Am J Physiol* 265:G775–G782.

- Greiner B, Eichelbaum M, Fritz P, Kreichgauer HP, von Richter O, Zundler J, and Kroemer HK (1999) The role of intestinal P-glycoprotein in the interaction of digoxin and rifampin. *J Clin Invest* 104:147–153.
- Lawrence JR, Sumner DJ, Kalk WJ, Ratcliffe WA, Whiting B, Gray K, and Lindsay M (1977) Digoxin kinetics in patients with thyroid dysfunction. *Clin Pharmacol Ther* 22:7–13.
- Li X, Misik AJ, Rieder CV, Solaro RJ, Lowen A, and Fliegel L (2002) Thyroid hormone receptor  $\alpha_1$  regulates expression of the Na<sup>+</sup>/H<sup>+</sup> exchanger (NHE1). *J Biol Chem* 277:28656–28662.
- Masuda S, Uemoto S, Hashida T, Inomata Y, Tanaka K, and Inui K (2000) Effect of intestinal P-glycoprotein on daily tacrolimus trough level in a living-donor small bowel recipient. *Clin Pharmacol Ther* 68:98–103.
- Matosin-Matekalo M, Mesonero JE, Laroche TJ, Lacasa M, and Brot-Laroche E (1999) Glucose and thyroid hormone co-regulate the expression of the intestinal fructose transporter GLUT5. *Biochem J* 339:233–239.
- O'Connor P and Feely J (1987) Clinical pharmacokinetics and endocrine disorders—therapeutic implications. *Clin Pharmacokinetics* 13:345–364.
- Ogihara H, Saito H, Shin BC, Terada T, Takenoshita S, Nagamachi Y, Inui K, and Takata K (1996) Immunolocalization of H<sup>+</sup> peptide cotransporter in rat digestive tract. *Biochem Biophys Res Commun* 220:848–852.
- Okamura N, Hirai M, Tanigawara Y, Tanaka K, Yasuhara M, Ueda K, Komano T, and Hori R (1993) Digoxin-cyclosporin A interaction: modulation of the multidrug transporter P-glycoprotein in the kidney. *J Pharmacol Exp Ther* 266:1614–1619.
- Ribeiro RCJ, Apriletti JW, West BL, Wagner RL, Fletcher RJ, Schaufele F, and Baxter JD (1995) The molecular biology of thyroid hormone action. *Ann NY Acad Sci* 758:366–389.
- Shenfield GM (1981) Influence of thyroid dysfunction on drug pharmacokinetics. *Clin Pharmacokinetics* 6:275–297.
- Shenfield GM, Thompson J, and Horn DB (1977) Plasma and urinary digoxin in thyroid dysfunction. *Eur J Clin Pharmacol* 12:437–443.
- Siegmund W, Altmannsberger S, Paneitz A, Hecker U, Zschiesche M, Franke G, Meng W, Warzok R, Schroeder E, Sperker B, et al. (2002) Effect of levothyroxine administration on intestinal P-glycoprotein expression: consequences for drug disposition. *Clin Pharmacol Ther* 72:256–264.
- Tanigawara Y, Okamura N, Hirai M, Yasuhara M, Ueda K, Kioka N, Komano T, and Hori R (1992) Transport of digoxin by human P-glycoprotein expressed in a porcine kidney epithelial cell line (LLC-PK<sub>1</sub>). *J Pharmacol Exp Ther* 263:840–845.
- Wakasugi H, Yano I, Ito T, Hashida T, Futami T, Nohara R, Sasayama S, and Inui K (1998) Effect of clarithromycin on renal excretion of digoxin: interaction with P-glycoprotein. *Clin Pharmacol Ther* 64:123–128.
- Yu DK (1999) The contribution of P-glycoprotein to pharmacokinetic drug-drug interactions. *J Clin Pharmacol* 39:1203–1211.
- Zhang F, Riley J, and Gant TW (1996) Use of internally controlled reverse transcriptase-polymerase chain reaction for absolute quantitation of individual multidrug resistant gene transcripts in tissue samples. *Electrophoresis* 17:255–260.
- Zhao JY, Ikeguchi M, Eckersberg T, and Kuo MT (1993) Modulation of multidrug resistance gene expression by dexamethasone in cultured hepatoma cells. *Endocrinology* 133:521–528.

Address correspondence to: Professor Ken-ichi Inui, Department of Pharmacy, Kyoto University Hospital, Sakyo-ku, Kyoto 606-8507, Japan. E-mail: inui@kuhp.kyoto-u.ac.jp



## Regulation of human peptide transporter 1 (PEPT1) in gastric cancer cells by anticancer drugs

Mayumi Inoue, Tomohiro Terada, Masahiro Okuda, Ken-ichi Inui\*

*Department of Pharmacy, Faculty of Medicine, Kyoto University Hospital, Kyoto University, Sakyo-ku, Kyoto 606-8507, Japan*

Received 25 October 2004; received in revised form 15 December 2004; accepted 18 December 2004

### Abstract

Human peptide transporter 1 (PEPT1) mediates the cellular uptake of di- and tripeptides and peptide-like drugs in the small intestine. In the present study, we examined the regulation of PEPT1 by anticancer drugs in the gastric cancer cell line MKN45. PEPT1 was expressed and functioned in MKN45 cells. The transport activity and mRNA expression of the facilitative glucose transporter 1 (GLUT1) were significantly decreased by 5-fluorouracil treatment, but those of PEPT1 were slightly increased. Cisplatin treatment affected neither PEPT1 nor GLUT1 activity. In conclusion, PEPT1 expressed in MKN45 cells are resistant against the cellular injury induced by 5-fluorouracil and cisplatin.

© 2005 Elsevier Ireland Ltd. All rights reserved.

*Keywords:* Peptide transporter; Gastric cancer; 5-Fluorouracil; Cisplatin

### 1. Introduction

The consumption of nutrients such as glucose and amino acids is augmented in cancer cells to meet the rapid metabolic turnover. Accordingly, following malignant transformation, the expression and function of several nutrient transporters are expected to be activated in order to increase the accumulation of nutrients.

Human peptide transporter 1 (PEPT1) is normally expressed in the small intestine and kidney and

mediates the transport of di- and tripeptides using the  $H^+$ -gradient as a driving force. PEPT1 also plays important roles as a drug transporter to mediate the transport of peptide-like drugs such as  $\beta$ -lactam antibiotics and the anticancer drug bestatin [1]. Previously, it was reported that PEPT1 is expressed in some human cancer cell lines such as AsPC-1 and Capan-2 (pancreatic cancer) [2] and SK-ChA-1 (cholangiocarcinoma) [3]. Using the broad substrate specificity of PEPT1, the development of selective drug delivery systems to cancer cells has been attempted [4]. For example, Neumann et al. [5] demonstrated that the endogenous photosensitizer  $\delta$ -aminolevulinic acid is accumulated specifically in bile duct tumor cells before photodynamic therapy. These findings suggest that PEPT1 may be

\* Corresponding author. Tel.: +81 75 751 3577; fax: +81 75 751 4207.

*E-mail address:* [inui@kuhp.kyoto-u.ac.jp](mailto:inui@kuhp.kyoto-u.ac.jp) (K. Inui).

a promising candidate for the delivery of anticancer drugs to cancer cells.

It has been demonstrated that various factors affect the transport activity of PEPT1 [6]. For example, PEPT1 is regulated by pharmacological agents, such as anticancer drugs, 5-fluorouracil (5-FU) [7] and cyclophosphamide [8], an agonist for  $\alpha_2$ -adrenergic receptor, clonidine [9], and a selective  $\sigma$ -receptor ligand, pentazocine [10]. However, there is little information about the regulation of human PEPT1 in cancer cells. Elucidation of the regulation of human PEPT1 in cancer cells by anticancer drugs may be essential for developing a drug delivery system targeting PEPT1.

Gastric cancer is one of the most frequent cancer in the world. The characterization of the cellular pathophysiology of gastric cancers is important for diagnosis, treatment and prevention, and numerous studies about gene expression profiles of gastric cancer have been performed [11,12]. However, the expression and functional characterization of PEPT1 in gastric cancer cells have not been clarified. In the present study, therefore, we examined the expression and function of PEPT1 in the gastric cancer cell line MKN45. Furthermore, the effects of 5-FU and cisplatin (CDDP) on PEPT1 and, as a comparison, those on facilitative glucose transporter 1 (GLUT1) were examined in MKN45 cells. Both drugs are frequently used for treating advanced gastric cancer.

## 2. Materials and methods

### 2.1. Agents

[<sup>3</sup>H]Glycylsarcosine and 2-deoxy-D-[<sup>3</sup>H]glucose were purchased from Moravek (Mercury Lane, Brea, CA) and Amersham (Buckinghamshire, England), respectively. Cefitibuten and cephalexin were kindly provided by Sionogi and Co. (Osaka, Japan). Cefadroxil was from Bristol Meyers Co. (Tokyo, Japan). Cyclacillin and cefotiam were from Takeda Chemical Industries (Osaka, Japan). Valacyclovir was from GlaxoSmithKline Research and Development (Hertfordshire, UK). Bestatin was from Nippon Kayaku (Tokyo, Japan). Glycine and 5-fluorouracil were obtained from Nacalai Tesque, Inc.

(Kyoto, Japan). Glycylsarcosine, ampicillin and cisplatin were purchased from Sigma Chemical Co. (St Louis, MO). All other chemicals used were of the highest purity available.

### 2.2. Gastric cancer cell lines

The human gastric cancer cell line MKN45 was obtained from Health Science Research Resources Bank (Osaka, Japan). MKN45 cells were cultured at 37 °C in a humidified atmosphere of 5% CO<sub>2</sub> and 95% air and maintained in RPMI-1640 medium containing 10% fetal bovine serum. The cells were subcultured every 5–6 days using 0.02% EDTA and 0.05% trypsin, and medium was replaced every 2–3 days. Typically, the cells cultured for 6 days were used for uptake studies and expression analysis.

### 2.3. mRNA expression analysis

Total RNA was isolated from MKN45 cells using an RNeasy mini kit (Qiagen, Hilden, Germany) according to the manufacturer's instructions. The RNA was reverse-transcribed using SuperScript™II RT (Invitrogen, Grand Island, NY) and amplified using Taq DNA polymerase (TaKaRa, Otsu, Japan) and PEPT1-specific oligonucleotide primers. The primer sequences for PEPT1 (accession number NM\_005073) were as follows: forward, 5'-ACACAGTTTCTTTGGTTATCCC-3' (74–95 bp); reverse, 5'-ATGAGAGCAGGAGGAACCCCA-3' (661–682 bp). PCR reaction was performed as follows: after an initial denaturation at 95 °C for 1 min, followed by 35 cycles of 95 °C for 1 min, 55 °C for 1 min, and 72 °C for 1 min, and a final elongation at 72 °C for 10 min.

For quantification of the amounts of PEPT1, GLUT1 and GAPDH mRNA expression, the real-time PCR method was carried out using the ABI PRISM 7700 sequence detector (Applied Biosystems, Foster, CA). The primer-probe set used for PEPT1 was as follows: forward primer, 5'-ATTGTGTCGCTCTCCATTGTCTAC-3' (306–329 bp); reverse primer, 5'-ATGACCTCACAGACCACAACCAT-3' (367–389 bp); fluorescence probe, 5'-(6-Fam) TTGGACAAGCAGTCACCTCAGTAAGCTCCA (Tamra) (phosphate)-3' (334–363 bp). The primer-probe sets used for GLUT1 and GAPDH were Pre-developed TaqMan Assay Reagents

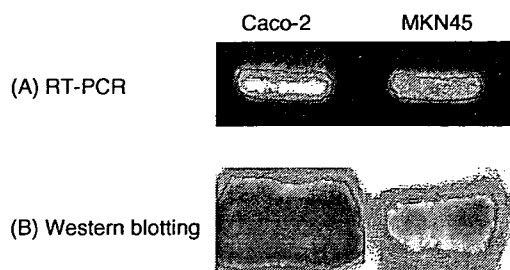


Fig. 1. PEPT1 mRNA (A) and protein (B) expression in MKN45 cells. As a positive control, Caco-2 cells on day 14 were used. (A) Total RNA (1  $\mu$ g) extracted from MKN45 or Caco-2 cells was reverse-transcribed and detected with specific oligonucleotide primers. (B) Crude membranes (70  $\mu$ g) from MKN45 cells and brush-border membranes (20  $\mu$ g) from Caco-2 cells were prepared and PEPT1 protein expression was detected by Western blotting using PEPT1-specific antibody.

(Applied Biosystems), and the reactions were performed according to the manufacturer's instructions. PCR amplification was performed with 2.5 ng of cDNA sample.

#### 2.4. Western blot analysis

The crude membrane fractions were prepared from MKN45 cells and Western blot analysis was performed as described previously [13,14]. As a positive control, brush border membrane fractions prepared from Caco-2 cells were used. Rabbit anti human PEPT1 antibody was raised and characterized as described [15].

#### 2.5. Uptake study

The uptake of [ $^3$ H]glycylsarcosine ([ $^3$ H]Gly-Sar) and 2-deoxy-D-[ $^3$ H]glucose (2[ $^3$ H]DG) by MKN45 cells was examined according to our previous studies [16]. In the case of 2[ $^3$ H]DG uptake, uptake medium not containing D-glucose was used. MKN45 cells were seeded on 12-well plate at a cell density of  $1 \times 10^5$  cells per well. The protein content of cell monolayers solubilized in 1 N NaOH was determined by the method of Bradford [17], using a Bio-Rad protein assay kit (Bio-Rad, Richmond, CA) with bovine  $\gamma$ -globulin as a standard.

#### 2.6. 5-FU and CDDP treatment of MKN45 cells

At 3 days after seeding, MKN45 cells were exposed to 5-FU or CDDP at the concentrations and for the periods indicated in the figures. Both 5-FU and CDDP were dissolved with dimethylsulfoxide (DMSO). The final concentration of DMSO in the treatment medium was 0.1%. The treatment medium was exchanged every 24 h.

#### 2.7. Statistical analysis

Results were expressed in the figures as the mean  $\pm$  SE. Data were analyzed with a nonpaired *t*-test or a one-way analysis of variance followed by Scheffe's test.

### 3. Results

PEPT1 mRNA was detected in MKN45 cells by RT-PCR analysis (Fig. 1), and Western blot analysis also showed PEPT1 protein expression in MKN45 cells (Fig. 1). These findings suggested that PEPT1 was expressed in gastric cancer cells.

To confirm the functional properties of PEPT1 in MKN45 cells, we further assessed the transport

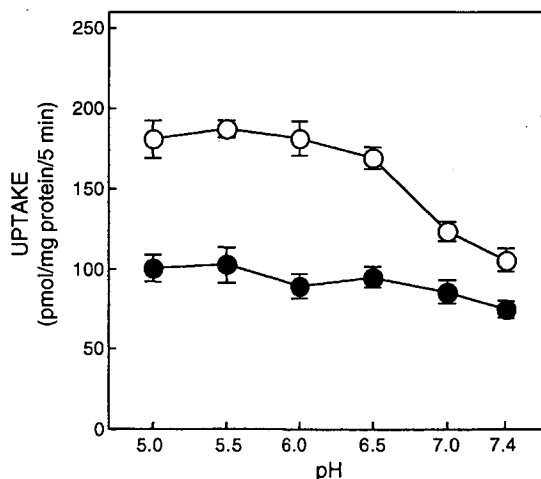


Fig. 2. Dependence on pH of [ $^3$ H]Gly-Sar uptake by MKN45 cells. The cells were incubated for 5 min at 37  $^{\circ}$ C at various pH with [ $^3$ H]Gly-Sar (50  $\mu$ M) in the absence (O) or presence (●) of 5 mM glycylsarcosine in incubation medium. Each point represents the mean  $\pm$  SE for three monolayers from a typical experiment.

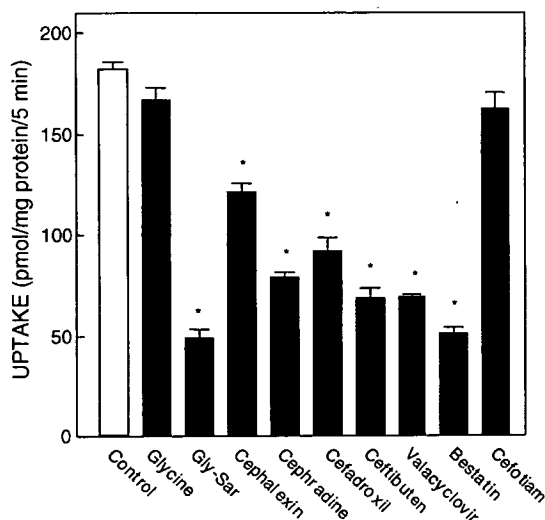


Fig. 3. Effects of various peptide-like drugs on [ $^3\text{H}$ ]Gly-Sar uptake by MKN45 cells. The cells were incubated for 5 min at 37 °C with [ $^3\text{H}$ ]Gly-Sar (50  $\mu\text{M}$ ) in the absence ( $\square$ ) or presence ( $\blacksquare$ ) of 10 mM of each drug in incubation medium (pH 6.0). Each column represents the mean  $\pm$  SE for three monolayers from a typical experiment. \* $P < 0.01$ , significantly different from control.

characteristics of [ $^3\text{H}$ ]Gly-Sar. [ $^3\text{H}$ ]Gly-Sar uptake by MKN45 cells was maximal at around pH 5.5 (Fig. 2), and significantly inhibited in the presence of excess PEPT1 substrates such as cephradine and bestatin, but not by glycine and cefotiam, which were not transported by PEPT1 (Fig. 3). We then examined the concentration dependence of [ $^3\text{H}$ ]Gly-Sar uptake by MKN45 cells. As shown in Fig. 4, Eadie–Hofstee plot analysis suggested that a single transporter was involved in MKN45 cells. The Michaelis–Menten constant ( $K_m$ ) value and the maximum uptake rates ( $V_{\max}$ ) were calculated to be  $1.56 \pm 0.24$  mM, and  $4.17 \pm 0.19$  nmol mg protein $^{-1}$  min $^{-1}$ , respectively, from three separate experiments. These characteristics of Gly-Sar transport are similar to those of transport by PEPT1 [1].

To examine whether the transport activity of PEPT1 was altered by anticancer drugs, we compared the uptake of [ $^3\text{H}$ ]Gly-Sar and 2[ $^3\text{H}$ ]DG, a substrate of GLUT1, after treatment with 5-FU and CDDP in MKN45 cells. [ $^3\text{H}$ ]Gly-Sar transport was significantly increased by the treatment with 1 and 5  $\mu\text{g}/\text{mL}$  of 5-FU for 72 h, but 2[ $^3\text{H}$ ]DG transport was markedly decreased by 5-FU treatment in a concentration and time-dependent manner (Fig. 5). On the other hand,

CDDP at 0.5–5  $\mu\text{g}/\text{mL}$  did not alter the [ $^3\text{H}$ ]Gly-Sar and 2[ $^3\text{H}$ ]DG transport (Fig. 6). We then treated MKN45 cells with 5-FU alone (1  $\mu\text{g}/\text{mL}$ ), CDDP alone (1  $\mu\text{g}/\text{mL}$ ) and the two agents combined (5-FU, 1  $\mu\text{g}/\text{mL}$ ; CDDP, 1  $\mu\text{g}/\text{mL}$ ), because both drugs are simultaneously administered to patients with FP therapy in clinical situations. As shown in Fig. 7, the effect of simultaneous treatment of 5-FU and CDDP on PEPT1 and GLUT1 was similar to that of 5-FU treatment alone, suggesting no additive effect of the two drugs on PEPT1 activity.

Next, we examined the mRNA expression level on 5-FU treatment using the real-time PCR method. We treated MKN45 cells with 10  $\mu\text{g}/\text{mL}$  of 5-FU for 72 h, because these conditions had the greatest effect on the cells as assessed in terms of cellular protein content (Fig. 8). As shown in Fig. 9, mRNA expression of GLUT1 and GAPDH in 5-FU treated cells were significantly reduced, but that of PEPT1 was slightly increased. We also found that PEPT1 protein was significantly increased by 5-FU treatment (Fig. 10). These results were consistent with the findings that

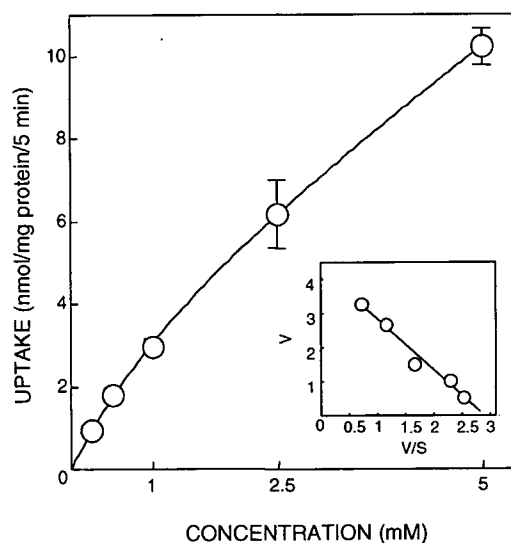


Fig. 4. Concentration-dependence of [ $^3\text{H}$ ]Gly-Sar uptake by MKN45 cells. The cells were incubated for 5 min at 37 °C with various concentrations of [ $^3\text{H}$ ]Gly-Sar in the incubation medium (pH 6.0). Each point represents the mean  $\pm$  SE for three monolayers from a typical experiment. Insets: Eadie–Hofstee plots of Gly-Sar uptake.  $V$ , uptake rate (nmol mg protein $^{-1}$  5 min $^{-1}$ );  $S$ , Gly-Sar concentration (mM). Each point represents the mean  $\pm$  SE for three monolayers from a typical experiment.



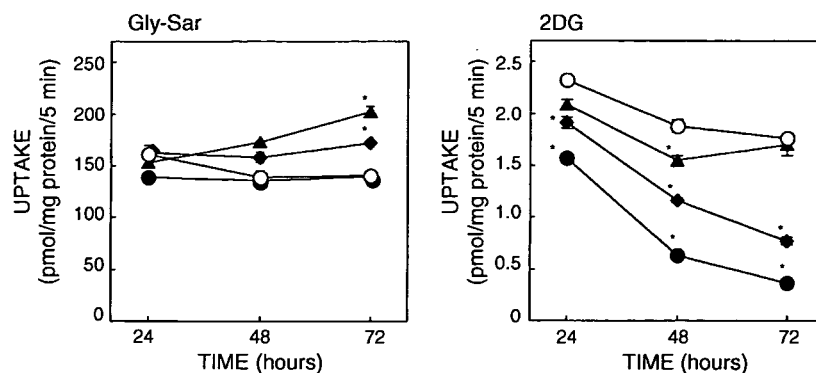


Fig. 5. Effect of 5-FU treatment on [ $^3\text{H}$ ]Gly-Sar and 2[ $^3\text{H}$ ]DG uptake by MKN45 cells. The cells were cultured with RPMI medium containing different concentrations of 5-FU (1  $\mu\text{g}/\text{mL}$  ( $\blacktriangle$ ), 5  $\mu\text{g}/\text{mL}$  ( $\blacklozenge$ ), and 10  $\mu\text{g}/\text{mL}$  ( $\bullet$ )), and 0.1% DMSO as a control (O). After 24–72 h treatment with 5-FU, uptake activity of PEPT1 and GLUT1 was examined with [ $^3\text{H}$ ]Gly-Sar (50  $\mu\text{M}$ ) and 2[ $^3\text{H}$ ]DG (71.4 nM), respectively. Each point represents the mean  $\pm$  SE for three monolayers from a typical experiment. \* $P < 0.01$ , significantly different from control in each period.

PEPT1 activity was maintained in spite of a decrease in cellular protein. It is, therefore, suggested that the level of PEPT1 protein per living cell increased during the treatment with 5-FU.

#### 4. Discussion

In the present study, we have demonstrated that PEPT1 is functionally expressed in MKN45 cells. Because PEPT1 is not expressed in the normal stomach, the expression of PEPT1 in MKN45 cells may be induced by malignant transformation.

PEPT1 was also expressed in pancreatic cancer cells such as AsPC-1 and Capan-2 [2] and the cholangiocarcinoma cell line SK-ChA-1 [3]. It is, therefore, speculated that high levels of PEPT1 may provide cancer cells with a metabolic advantage. Alterations of nutrient transporters in cancer cells have been used for diagnosis or treatment. For example, positron emission tomography (PET) using [ $^{18}\text{F}$ ]-2-fluoro-2-deoxy-D-glucose (FDG) has been widely used in the non-invasive imaging of malignancies, based on the altered uptake of glucose mediated by overexpressed GLUT1 in cancer cells [18,19]. Furthermore, as a candidate for target

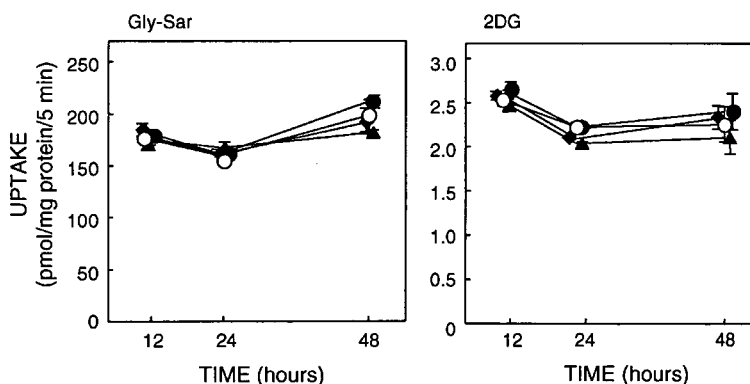


Fig. 6. Effect of CDDP treatment on [ $^3\text{H}$ ]Gly-Sar and 2[ $^3\text{H}$ ]DG uptake by MKN45 cells. The cells were incubated with RPMI medium containing different concentrations of CDDP (0.5  $\mu\text{g}/\text{mL}$  ( $\blacktriangle$ ), 1  $\mu\text{g}/\text{mL}$  ( $\blacklozenge$ ), and 5  $\mu\text{g}/\text{mL}$  ( $\bullet$ )), and 0.1% DMSO as a control (O). After 12–48 h treatment with CDDP, uptake activity of PEPT1 and GLUT1 was examined with [ $^3\text{H}$ ]Gly-Sar (50  $\mu\text{M}$ ) and 2[ $^3\text{H}$ ]DG (71.4 nM), respectively. Each point represents the mean  $\pm$  SE for three monolayers from a typical experiment. \* $P < 0.01$ , significantly different from control in each period.

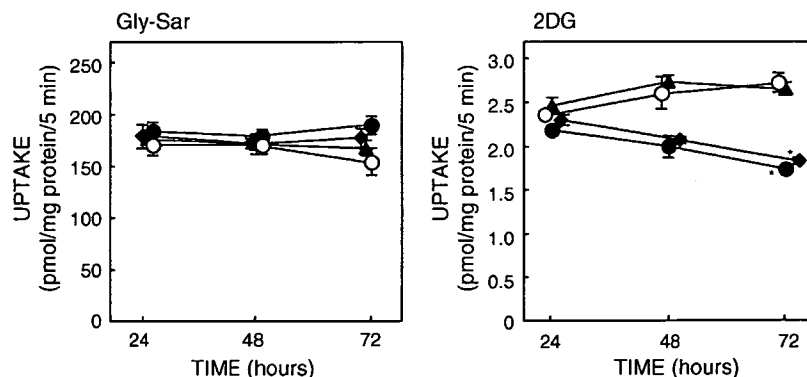


Fig. 7. Effect of simultaneous treatment with 5-FU and CDDP on  $[^3\text{H}]\text{Gly-Sar}$  and  $2[^3\text{H}]\text{DG}$  uptake by MKN45 cells. The cells were incubated with RPMI medium containing 5-FU ( $1\ \mu\text{g}/\text{mL}$ ) ( $\blacklozenge$ ), CDDP ( $1\ \mu\text{g}/\text{mL}$ ) ( $\blacktriangle$ ), 5-FU ( $1\ \mu\text{g}/\text{mL}$ ) + CDDP ( $1\ \mu\text{g}/\text{mL}$ ) ( $\bullet$ ) and 0.1% DMSO as a control ( $\circ$ ). After 24–72 h treatment, uptake activity of PEPT1 and GLUT1 was examined with  $[^3\text{H}]\text{Gly-Sar}$  ( $50\ \mu\text{M}$ ) and  $2[^3\text{H}]\text{DG}$  ( $71.4\ \text{nM}$ ), respectively. Each point represents the mean  $\pm$  SE for 12 monolayers from four separate experiments ( $[^3\text{H}]\text{Gly-Sar}$ ) and three monolayers ( $2[^3\text{H}]\text{DG}$ ). \* $P < 0.01$ , significantly different from control in each period.

molecules for cancer therapy, transporter molecules have been widely investigated. For example, Noguchi et al. [20] demonstrated that the suppression of GLUT1 mRNA using an antisense method resulted in a decrease in tumor growth, and Fuchs et al. [21] reported that antisense RNA targeting an amino acid transporter ( $\text{ATB}^0/\text{ASCT2}$ ) elicits apoptosis. As to PEPT1, the development of a drug delivery system targeting cancer cells has been attempted [4,5]. At present, it is not clear how PEPT1 is regulated in cancer cells, but the elucidation of signal pathways to induce the expression of PEPT1 may provide useful information on the cellular physiology of cancer cells and for the target strategy of anticancer drugs utilizing PEPT1.

5-FU is one of the most effective anticancer drugs and used in chemotherapy against a variety of solid tumors including gastric cancer [22]. It has been demonstrated that 5-FU altered the expression of various genes such as the p53 [23] and inducible nitric oxide synthase [24] in gastric cancer cells, and that these alterations may contribute to the pharmacological effects of 5-FU. Although 5-FU-based chemotherapy improves survival, drug resistance remains a significant limitation to the clinical use of 5-FU. The present study also showed that GLUT1 and GAPDH levels in MKN45 cells were significantly decreased by 5-FU treatment. In contrast, the function and expression of PEPT1 in living cells were enhanced

by 5-FU treatment, suggesting that the supply of small peptides for MKN45 cells was maintained in spite of 5-FU-induced cell injury. Although the exact mechanisms responsible for the resistance of PEPT1 to

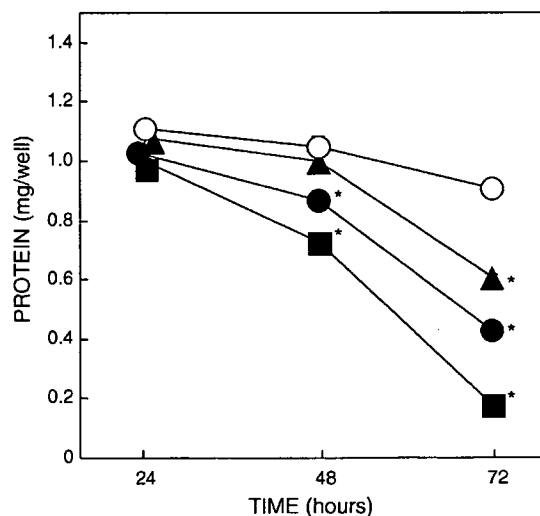


Fig. 8. Effect of 5-FU on cellular protein content in MKN45 cells. The cells were cultured with RPMI medium containing different concentrations of 5-FU ( $1\ \mu\text{g}/\text{mL}$ ) ( $\blacktriangle$ ),  $5\ \mu\text{g}/\text{mL}$ ) ( $\blacklozenge$ ), and  $10\ \mu\text{g}/\text{mL}$ ) ( $\blacksquare$ ), and 0.1% DMSO as a control ( $\circ$ ). After 24–72 h treatment with 5-FU, the protein contents were measured. Each point represents the mean  $\pm$  SE for three monolayers from a typical experiment. \* $P < 0.01$ , significantly different from control in each period.

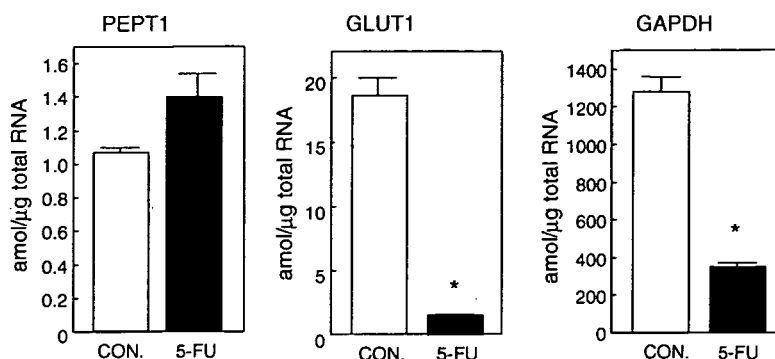


Fig. 9. Effects of 5-FU on the amount of PEPT1, GLUT1 and GAPDH mRNA expression by MKN45 cells. After the cells were cultured with RPMI medium containing 5-FU (10  $\mu\text{g}/\text{mL}$ ) for 72 h, total RNA was extracted and reverse-transcribed. For real-time PCR, 2.5 ng cDNA samples were analyzed with specific oligonucleotide primers and TaqMan probes. Each column represents the mean  $\pm$  SE for three monolayers from a typical experiment. \* $P < 0.01$ , significantly different from control.

5-FU are unclear, the increased stability of PEPT1 mRNA and protein or some stress-induced factors may be involved. Similarly, it has been demonstrated that the function of PEPT1 was resistant to cell damage caused by starvation [25,26], and the administration of 5-fluorouracil (5-FU) [7], and cyclophosphamide [8]. These findings suggested that PEPT1 is resistant to severe stress. Because FDG uptake during PET increased depending on the expression of GLUT1, apparent anti-tumor effects of anticancer drugs such as 5-FU may be assessed based on decreased GLUT1 activity. But considering the clinical effects of 5-FU, an assessment of chemotherapy based only on GLUT1 may not be enough because a sustained supply of peptides and other nutrients results in cell survival. Some poorly differentiated colon and gastric cancer cell lines including MKN45 cells are reported to be survived in cultures not containing glucose and amino acids [27]. In this way, the resistance of tumor cells to glucose and amino acid deprivation may relate to the metabolism of other nutrients such as small peptides. Our study could suggest that ectopic PEPT1 activity and resistance to severe conditions in some gastric cancer cells enhances cell survival, and PEPT1 has the capacity to become a target molecule from the viewpoint of drug discovery and delivery.

In conclusion, our findings showed that PEPT1 is expressed and functioned in MKN45 cells. The function of PEPT1 was unaffected by the cellular injury induced by 5-FU treatment. Further studies

concerning the pathophysiological role of PEPT1 in cancer cells and regulatory mechanisms of PEPT1 should facilitate the development of effective chemotherapeutics.

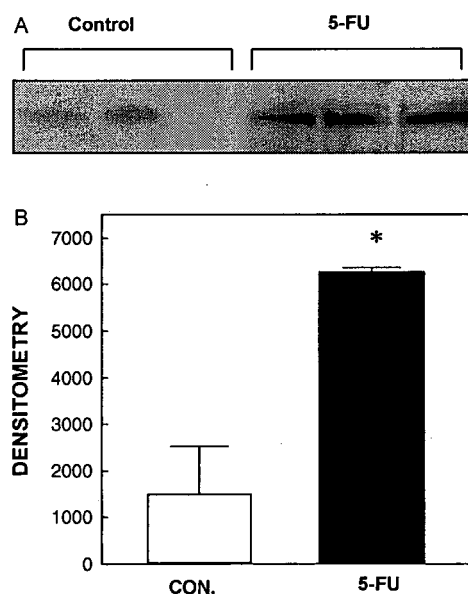


Fig. 10. Effect of 5-FU on the amount of PEPT1 protein expression by MKN45 cells. (A) After the cells were cultured with RPMI medium containing 5-FU (10  $\mu\text{g}/\text{mL}$ ) for 72 h, crude membrane was prepared, and PEPT1 protein expression was detected by Western blotting using PEPT1-specific antibody. Cell lysates, 50  $\mu\text{g}$  each, were loaded into each lane. (B) PEPT1 protein levels were quantified by scanning densitometry. Each column represents the mean  $\pm$  SE of three monolayers from a typical experiment. \* $P < 0.01$ , significantly different from control.

## Acknowledgements

This work was supported in part by a Grant-in-Aid for Scientific Research from the Ministry of Education, Culture, Sports, Science and Technology of Japan.

## References

- [1] T. Terada, K. Inui, Peptide transporters: structure, function, regulation and application for drug delivery, *Curr. Drug Metab.* 5 (2004) 85–94.
- [2] D.E. Gonzalez, K.M. Covitz, W. Sadee, R.J. Mrsny, An oligopeptide transporter is expressed at high levels in the pancreatic carcinoma cell lines AsPc-1 and Capan-2, *Cancer Res.* 58 (1998) 519–525.
- [3] I. Knutter, I. Rubio-Aliaga, M. Boll, G. Hause, H. Daniel, K. Neubert, M. Brandsch, H<sup>+</sup>-peptide cotransport in the human bile duct epithelium cell line SK-ChA-1, *Am. J. Physiol. Gastrointest. Liver Physiol.* 283 (2002) G222–G229.
- [4] T. Nakanishi, I. Tamai, A. Takaki, A. Tsuji, Cancer cell-targeted drug delivery utilizing oligopeptide transport activity, *Int. J. Cancer* 88 (2000) 274–280.
- [5] J. Neumann, M. Brandsch,  $\delta$ -aminolevulinic acid transport in cancer cells of the human extrahepatic biliary duct, *J. Pharmacol. Exp. Ther.* 305 (2003) 219–224.
- [6] S.A. Adibi, Regulation of expression of the intestinal oligopeptide transporter (Pept-1) in health and disease, *Am. J. Physiol. Gastrointest. Liver Physiol.* 285 (2003) G779–G788.
- [7] H. Tanaka, K.I. Miyamoto, K. Morita, H. Haga, H. Segawa, T. Shiraga, et al., Regulation of the PepT1 peptide transporter in the rat small intestine in response to 5-fluorouracil-induced injury, *Gastroenterology* 114 (1998) 714–723.
- [8] J. Satoh, T. Tsujikawa, Y. Fujiyama, T. Bamba, Nutritional benefits of enteral alanyl-glutamine supplementation on rat small intestinal damage induced by cyclophosphamide, *J. Gastroenterol. Hepatol.* 18 (2003) 719–725.
- [9] F. Berlioz, J.J. Maoret, H. Paris, M. Laburthe, R. Farinotti, C. Roze,  $\alpha_2$ -adrenergic receptors stimulate oligopeptide transport in a human intestinal cell line, *J. Pharmacol. Exp. Ther.* 294 (2000) 466–472.
- [10] T. Fujita, Y. Majikawa, S. Umehisa, N. Okada, A. Yamamoto, V. Ganapathy, F.H. Leibach,  $\sigma$  Receptor ligand-induced up-regulation of the H<sup>+</sup>/peptide transporter PEPT1 in the human intestinal cell line Caco-2, *Biochem. Biophys. Res. Commun.* 261 (1999) 242–246.
- [11] K.F. Becker, G. Keller, H. Hoefler, The use of molecular biology in diagnosis and prognosis of gastric cancer, *Surg. Oncol.* 9 (2000) 5–11.
- [12] W. Yasui, N. Oue, R. Ito, K. Kuraoka, H. Nakayama, Search for new biomarkers of gastric cancer through serial analysis of gene expression and its clinical implications, *Cancer Sci.* 95 (2004) 385–392.
- [13] H. Saito, M. Okuda, T. Terada, S. Sasaki, K. Inui, Cloning and characterization of a rat H<sup>+</sup>/peptide cotransporter mediating absorption of  $\beta$ -lactam antibiotics in the intestine and kidney, *J. Pharmacol. Exp. Ther.* 275 (1995) 1631–1637.
- [14] T. Terada, H. Saito, M. Mukai, K. Inui, Identification of the histidine residues involved in substrate recognition by a rat H<sup>+</sup>/peptide cotransporter, PEPT1, *FEBS Lett.* 394 (1996) 196–200.
- [15] K. Ashida, T. Katsura, H. Motohashi, H. Saito, K. Inui, Thyroid hormone regulates the activity and expression of the peptide transporter PEPT1 in Caco-2 cells, *Am. J. Physiol. Gastrointest. Liver Physiol.* 282 (2002) G617–G623.
- [16] T. Terada, K. Sawada, H. Saito, Y. Hashimoto, K. Inui, Functional characteristics of basolateral peptide transporter in the human intestinal cell line Caco-2, *Am. J. Physiol.* 276 (1999) G1435–G1441.
- [17] M.M. Bradford, A rapid and sensitive method for the quantitation of microgram quantities of protein utilizing the principle of protein-dye binding, *Anal. Biochem.* 72 (1976) 248–254.
- [18] T. Kurokawa, Y. Yoshida, K. Kawahara, T. Tsuchida, H. Okazawa, Y. Fujibayashi, et al., Expression of GLUT-1 glucose transfer, cellular proliferation activity and grade of tumor correlate with [F-18]-fluorodeoxyglucose uptake by positron emission tomography in epithelial tumors of the ovary, *Int. J. Cancer* 109 (2004) 926–932.
- [19] M. Kunkel, T.E. Reichert, P. Benz, H.A. Lehr, J.H. Jeong, S. Wieand, et al., Overexpression of Glut-1 and increased glucose metabolism in tumors are associated with a poor prognosis in patients with oral squamous cell carcinoma, *Cancer* 97 (2003) 1015–1024.
- [20] Y. Noguchi, A. Saito, Y. Miyagi, S. Yamanaka, D. Marat, C. Doi, et al., Suppression of facilitative glucose transporter 1 mRNA can suppress tumor growth, *Cancer Lett.* 154 (2002) 175–182.
- [21] B.C. Fuchs, J.C. Perez, J.E. Suetterlin, S.B. Chaudhry, B.P. Bode, Inducible antisense RNA targeting amino acid transporter ATB<sup>0</sup>/ASCT2 elicits apoptosis in human hepatoma cells, *Am. J. Physiol. Gastrointest. Liver Physiol.* 286 (2004) G467–G478.
- [22] D.B. Longley, D.P. Harkin, P.G. Johnston, 5-fluorouracil: mechanisms of action and clinical strategies, *Nat. Rev. Cancer* 3 (2003) 330–338.
- [23] M. Osaki, S. Tatebe, A. Goto, H. Hayashi, M. Oshimura, H. Ito, 5-Fluorouracil (5-FU) induced apoptosis in gastric cancer cell lines: role of the p53 gene, *Apoptosis* 2 (1997) 221–226.
- [24] I.D. Jung, S.Y. Yang, C.G. Park, K.B. Lee, J.S. Kim, S.Y. Lee, et al., 5-Fluorouracil inhibits nitric oxide production through the inactivation of I $\kappa$ B kinase in stomach cancer cells, *Biochem. Pharmacol.* 64 (2002) 1439–1445.